PRELIMINARY PERMEABILITY AND WATER-RETENTION DATA FOR NONWELDED AND BEDDED TUFF SAMPLES, YUCCA MOUNTAIN AREA, NYE COUNTY, NEVADA

By Lorraine E. Flint, Raytheon Services of Nevada, and
Alan L. Flint, U.S. Geological Survey

U.S. GEOLOGICAL SURVEY

Open-File Report 90-569

Prepared in cooperation with the
NEVADA OPERATIONS OFFICE,
U.S. DEPARTMENT OF ENERGY, under
Interagency Agreement DE-AI08-78ET44802

Denver, Colorado
1990

U.S. DEPARTMENT OF THE INTERIOR

MANUEL LUJAN, JR., Secretary

U.S. GEOLOGICAL SURVEY

Dallas L. Peck, Director

For additional information
write to:

Chief, Yucca Mountain Project Branch
U.S. Geological Survey
Box 25046, Mail Stop 421
Denver Federal Center
Denver, CO 80225-0046

Copies of this report can
be purchased from:

U.S. Geological Survey
Books and Open-File Reports Section
Federal Center, Building 810
Box 25425
Denver, CO 80225-0425

CONTENTS

FIGURES

TABLES

CONVERSION FACTORS

Multiply	*By*	*To obtain*
bars	14.50	pounds per square inch (lb/in^2)
centimeter per second (cm/s)	0.03281	foot per second (ft/s)
centipoise (0.01 g/cm-s)	6.72E-4	pound per foot-second (lb/ft-s)
cubic centimeter (cm^3)	3.531E-5	cubic foot (ft^3)
cubic centimeter per second (cm^3/s)	3.531E-5	cubic foot per second (ft^3/s)
darcies (D)	1.05E-5	square foot (ft^2)
gram per cubic centimeter (gm/cm^3)	62.43	pound per cubic foot (lb/ft^3)
gram per liter (g/L)	0.008345	pound per gallon (lb/gal)
millidarcies (mD)	1.05E-8	square foot (ft^2)
millimeters (mm)	0.03937	inch (in.)
poise (1 g/cm-s)	6.72E-6	pound per foot-second (lb/ft-s)
radian per second (rad/s)	57.29	degree per second
square centimeter (cm^2)	0.001076	square foot (ft^2)

Temperature in degree Fahrenheit (°F) as follows:

$$°F = 9/5\ (°C) + 32$$

PRELIMINARY PERMEABILITY AND WATER-RETENTION DATA FOR NONWELDED AND BEDDED TUFF, YUCCA MOUNTAIN AREA, NYE COUNTY, NEVADA

By Lorraine E. Flint and Alan L. Flint

ABSTRACT

Measurements of rock-matrix hydrologic properties at Yucca Mountain, a potential site for a high-level nuclear waste repository, are needed to predict rates and direction of water flow in the unsaturated zone. The objective of this study is to provide preliminary data on intrinsic and relative permeability and moisture retention on rock core samples and to present the methods used to collect these data.

Four methods were used to measure intrinsic, or saturated permeability: Air, Klinkenberg, specific permeability to oil, and specific permeability to water. Two methods yielded data on relative permeability (gas-drive and centrifuge), and three methods (porous plate, centrifuge, and mercury intrusion porosimetry) were used to measure water-retention properties (matric potential compared to water-content curves). Standard measurements of grain density, bulk density, and porosity for the core samples were included.

Results of this study showed a large range of intrinsic permeability values among rock types and high variability within rock types. For example, permeability values for samples from the tuffaceous beds of Calico Hills (hereafter referred to as Calico Hills) were, on the average, three orders of magnitude smaller than all others. The four methods yield intrinsic permeability values that are different but are highly correlated (coefficient of determination greater than 0.94).

INTRODUCTION

Yucca Mountain, Nevada (fig. 1) is being studied as a potential site for a high-level radioactive waste repository. The U.S. Geological Survey is responsible for characterizing the hydrologic flow properties of the unsaturated zone matrix for the Matrix Hydrologic Properties program which is part of study plan entitled "Percolation of the Deep Unsaturated Zone."

The objective of this study is to present methods used for measuring intrinsic permeability, relative permeability, and water retention (matric potential compared to water content) on samples of rock core; and to provide data collected by these methods. Evaluations of these standard methods, most of which have been developed for application in the petroleum industry, eventually will be coupled with additional methods currently being developed for

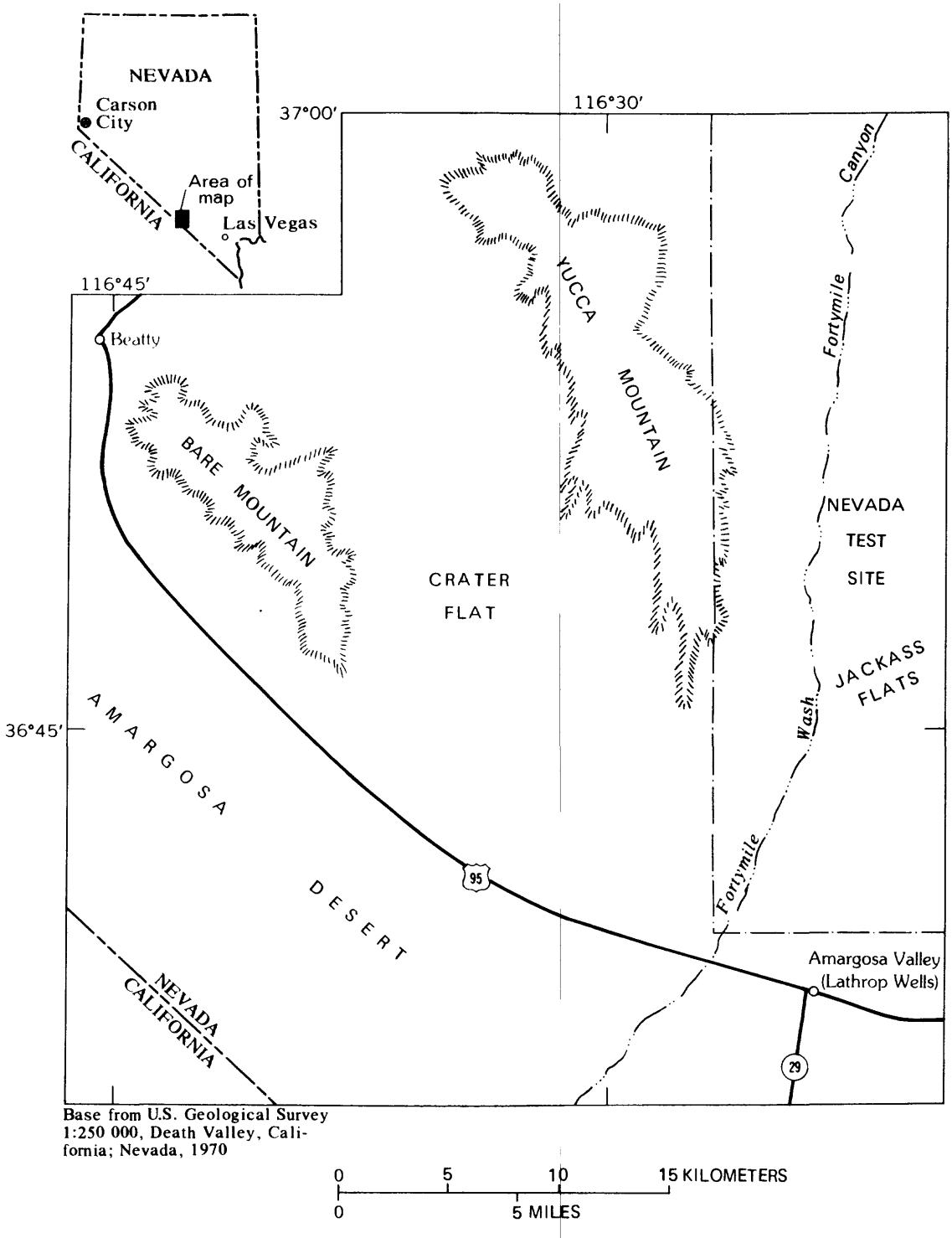

Figure 1.--Map of southern Nevada showing location of study area.

use in unsaturated-zone studies. The prototype methods are techniques or concepts commonly used in agriculture for soils, and the attempt is being made to adapt them for use on rock core samples. As part of this study, samples were collected from nonwelded and bedded tuffs. This report presents information on the permeability and water-retention characteristics of these samples.

Purpose and Scope

The purpose of this report is to provide preliminary data needed for the data bases used in the development of hydrologic models for the Yucca Mountain project. The methods used for collecting these data, standard laboratory-measurement techniques, also are presented in this report. Measurements of core grain density, bulk density, and porosity were made because these measurements are needed to define the characteristics of individual cores and supply information needed for the calculations of the hydrologic properties.

Core samples were obtained from nine boreholes (fig. 2) that penetrated various lithostratigraphic units of the late Tertiary Paintbrush Tuff and the Calico Hills (fig. 3). These were chosen for measurement to represent the possible range of permeability values that would be encountered. This would help define the methodology required to establish the upper and lower limits of permeability determination. The study was limited to samples of nonwelded tuffs that have large porosity values and relatively large saturated hydraulic-conductivity values compared to welded tuff.

Study Site and Sampling Locations

Yucca Mountain is an eastward-tilted volcanic plateau consisting of a thick sequence of ash-fall tuffs, pumice-fall tuffs, and reworked tuffs of late Tertiary age. Most of the ash-flow tuffs consist of welded, compositionally zoned, and compound cooling units, but nonwelded, compositionally homogeneous, or simple cooling units are also present. In addition, minor intervals of bedded tuffs are located between ash-flow tuff members or formations (Scott and Castellanos, 1984). Many of the tuffs also are diagenetically altered, containing zeolites, clays, and other minerals of secondary origin. In particular, smectite clays are closely associated with the zeolites in the altered tuffs. These clay minerals might interact with water and affect the permeability of the tuffs to water.

Seventy-three core samples were collected and analyzed. These samples were used to compare measurement methods and are listed in table 1. Samples were collected from boreholes (fig. 2) continuously cored using an air-coring method. Original cores were 6 cm in diameter and undercored to provide 2.5-cm-diameter vertical and horizontal cores for the matrix permeability tests. These vertical and horizontal cores were analyzed at Core Laboratories, Inc.[1], in Aurora, Colo. Two and five-tenths centimeter core samples were also analyzed by the U.S. Geological Survey petrophysics laboratory in Golden, Colo., and were undercored from adjacent 6-cm-diameter cores.

---

[1]The use of brand, trade, or firm names in this report is for identification purposes only and does not constitute endorsement by the U.S. Geological Survey, or impute responsibility for any present or potential effects on the natural resources.

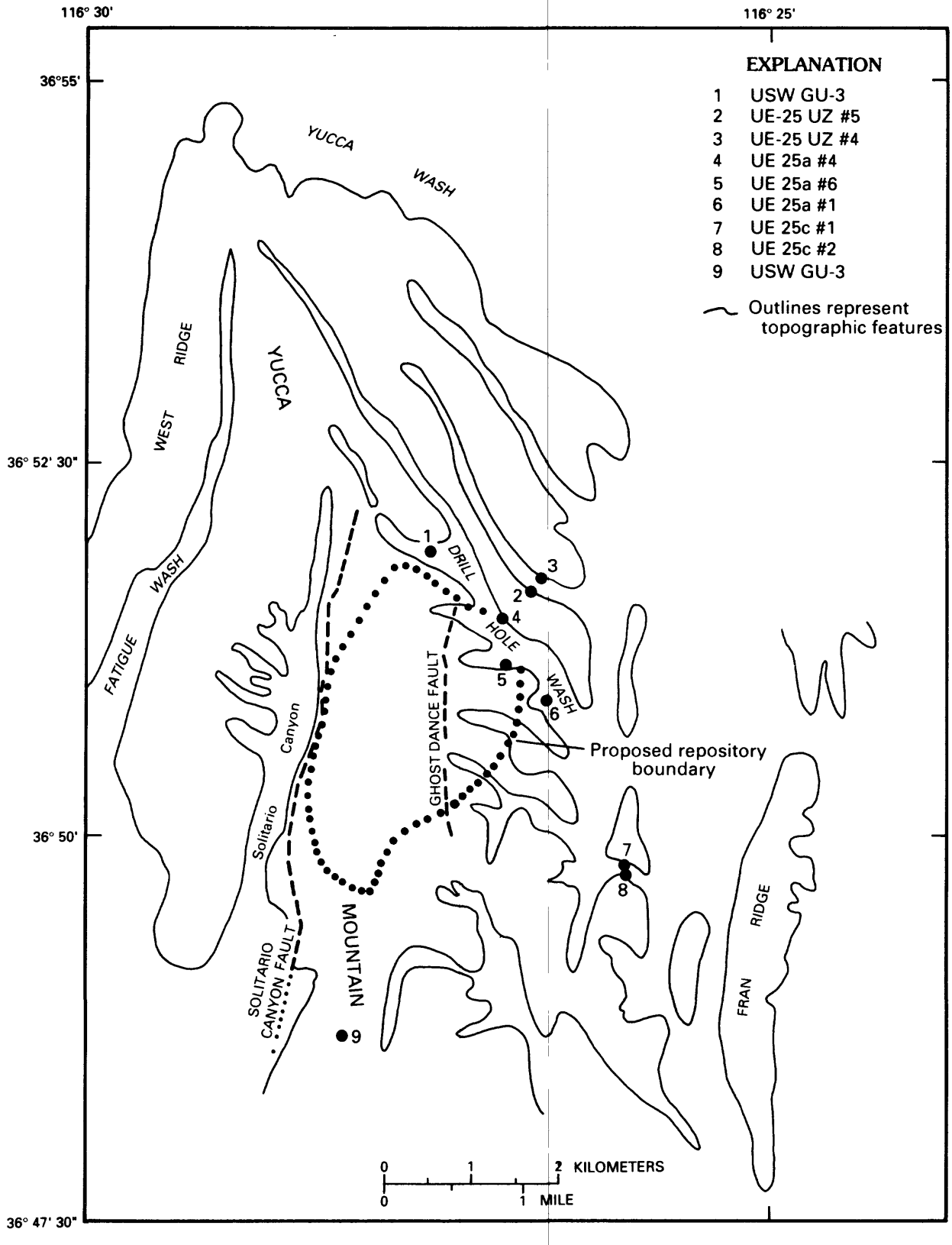

Figure 2.--Map of Yucca Mountain area showing location of boreholes from which core samples were obtained.

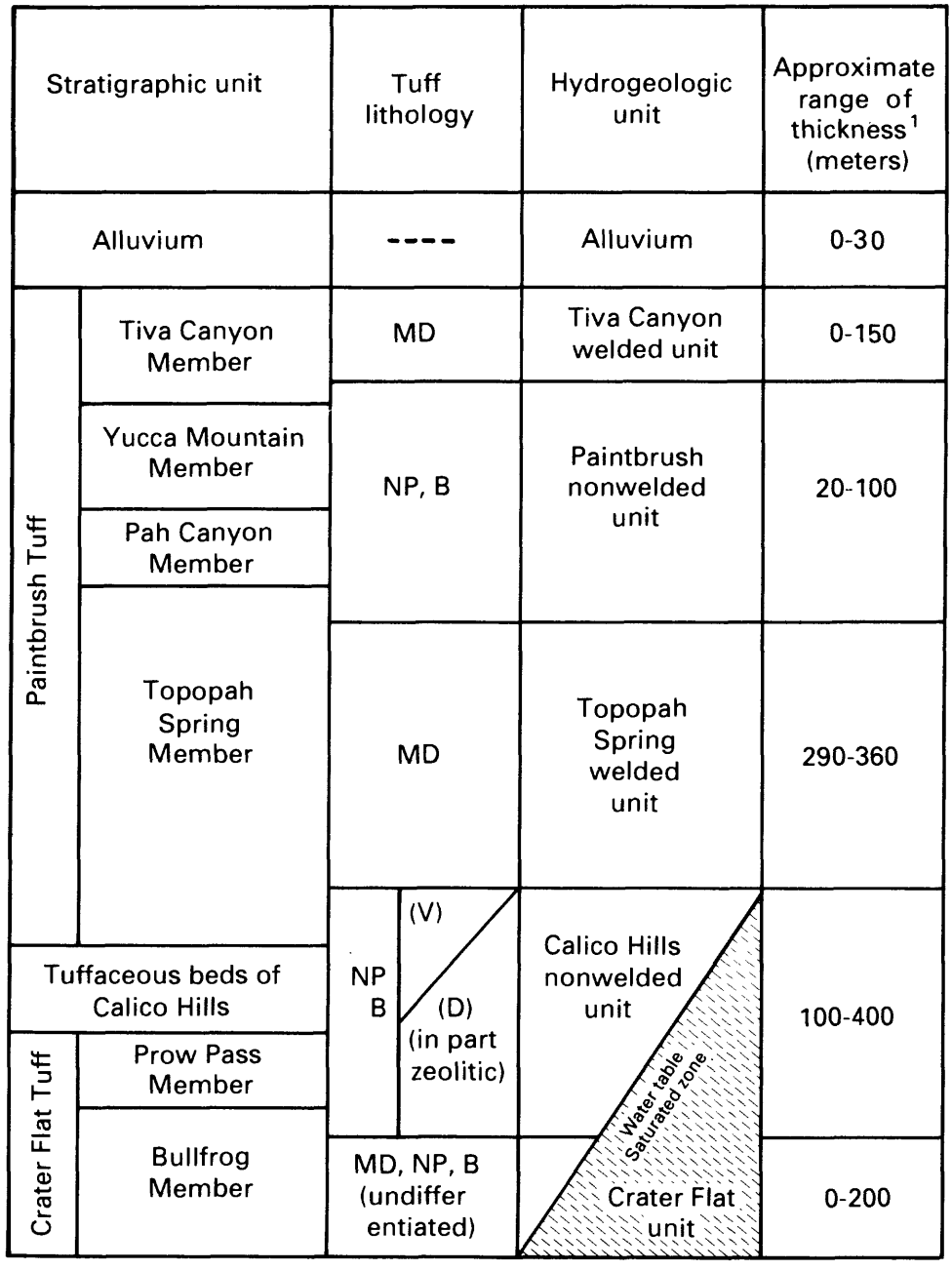

[1]Thicknesses from geologic sections of Scott and Bonk (1984).

Figure 3.--Idealized stratigraphic column showing relations between stratigraphic (geologic) units, lithology, and hydrogeologic units (from Montazer and Wilson, 1984).

Table 1.--*Sample identifications, locations, and descriptions*

["H" in sample ID indicates horizontally oriented core sample. All other samples are vertical. "P" indicates samples measured by U.S. Geological Survey petrophysics laboratory, Golden, Colo. All other samples measured by Core Laboratories, Aurora, Colo. Individual sample labels represent individual core samples.]

Sample label	Well or borehole (fig. 2)	Depth interval (meters)	Geologic unit	Core matrix description
1U,1UH	USW GU-3	432.36-432.51	Calico Hills	Vitric
2U,2UH	USW GU-3	456.96-457.20	Calico Hills	Vitric
1P,1PH	UE-25c #2	405.08-405.20	Calico Hills	Devitrified, zeolitized
2P,2PH	UE-25c #2	426.17-426.48	Calico Hills	Devitrified, zeolitized
3P,3PH	UE-25c #1	462.17-462.50	Calico Hills	Devitrified, zeolitized
20A,20AP	USW G-1	487.86-488.02	Calico Hills	Zeolitized
12A,12AP	USW G-1	535.50-535.66	Calico Hills	Zeolitized
13A,13AP	USW G-1	546.29-546.45	Calico Hills	Zeolitized
14A,14AP	USW G-1	573.12-573.27	Calico Hills	Zeolitized
16A,16AP	USW G-1	589.03-589.18	Calico Hills	Zeolitized
15A,15AP	USW G-1	623.83-623.99	Calico Hills	Zeolitized
17A,17AH,17AP	USW G-1	632.80-632.98	Calico Hills	Zeolitized
18A,18AH,18AP	USW G-1	660.99-661.14	Calico Hills	Zeolitized
19A,19AH,19AP	USW G-1	439.95-440.10	Calico Hills	Zeolitized, partially argillic
8A,8AP	USW G-1	505.39-505.54	Calico Hills	Zeolitized, partially argillic
11A,11AP	USW G-1	518.16-518.31	Calico Hills	Zeolitized, partially argillic
1A,1AP	USW G-1	544.25-544.40	Calico Hills	Zeolitized, partially argillic
7A,7AP	UE-25a #1	431.96-432.15	Calico Hills	Devitrified, slightly zeolitized
9A,9AH,9AP	UE-25a #1	470.92-471.10	Calico Hills	Vitric
10A,10AP	UE-25a #1	549.10-549.25	Bedded-reworked tuff	
4A,4AP	UE-25a #6	40.75-40.87	Base of Tiva Canyon Member	Vitric
5A,5AP	UE-25a #4	43.16-43.25	Base of Tiva Canyon Member	Vitric
2A,2AP	UE-25a #1	65.07-65.23	Base of Tiva Canyon Member	Vitric, partially argillic
6A,6AP	UE-25a #4	47.15-47.46	Yucca Mountain Member	Vitric
3A,3AH,3AP	UE-25a #4	47.79-47.98	Yucca Mountain Member	Vitric
IV,IVP	UE-25a #6	50.81-50.93	Yucca Mountain Member	Vitric
5-2,5-2H	UE-25 UZ #5	42.43-42.58	Yucca Mountain Member	Vitric
5-1B	UE-25 UZ #5	38.44-38.62	Yucca Mountain Member	Vitric
4-4,4-4H	UE-25 UZ #4	72.97-73.12	Pah Canyon Member	Vitric
4-5,4-5H	UE-25 UZ #4	84.49-84.64	Pah Canyon Member	Vitric
5-6	UE-25 UZ #5	70.65-40.33	Pah Canyon Member	Vitric
5-7	UE-25 UZ #5	79.74-79.89	Pah Canyon Member	Vitric
4-6,4-6H	UE-25 UZ #4	93.94-94.06	Bedded-reworked tuff	
4-7,4-7H	UE-25 UZ #4	101.68-101.83	Bedded-reworked tuff	
5-1	UE-25 UZ #5	32.28-32.43	Bedded-reworked tuff	
5-1A	UE-25 UZ #5	34.29-34.44	Bedded-reworked tuff	
5-8	UE-25 UZ #5	96.80-96.93	Bedded-reworked tuff	
5-9	UE-25 UZ #5	105.55-105.64	Topopah Spring Member	Vitric

Definitions and Relations Between Properties

The following section defines the properties that were measured for the core samples. Relations between calculated and measured values also are discussed.

Core Physical Properties

Physical properties are those defining mass and volume relations. Grain density, ρ_s, is defined as the mass of the solids, M_s, divided by the volume of the solids, V_s. Dry bulk density, ρ_b, is M_s divided by the volume of the total sample, V_t (solids and pores together). Porosity is the relative pore volume in the soil or core, or the volume of air plus water divided by V_t. Porosity, ϕ, is calculated in cm^3/cm^3 as:

$$\phi = 1 - (\rho_b/\rho_s). \quad (1)$$

Porosity is the fractional volume of water and air that a given volume of soil or rock can accommodate.

Intrinsic Permeability and Saturated Hydraulic Conductivity

Permeability (or intrinsic permeability) is the capacity of a porous medium for transmitting fluid. Permeability is a property of the porous medium and its pore geometry alone, which includes factors such as size, shape, and distribution and tortuosity of pores. The measurement of intrinsic permeability is a measure of the fluid conductivity of the particular medium. If a porous body is not chemically inert and physically stable (nondeformable), there are matrix-water interactions such that fluid transmittance is best discussed in terms of hydraulic conductivity. Saturated hydraulic conductivity depends on the properties of the porous medium and the fluid. Permeability, k, is related to hydraulic conductivity, K, by:

$$k = K\eta/\rho g, \quad (2)$$

where η = dynamic viscosity of the fluid [Mass (M)/Length (L) * Time (T)],
ρ = density of the fluid (M/L^3), and
g = acceleration due to gravity (L/T^2).

Permeability measurements are necessary because attempts to establish empirical correlations between permeability and physical properties have been unsatisfactory. If permeability is determined using a specific liquid, such as the water occurring in the formation, then the specific intrinsic permeability to liquid and the hydraulic conductivity should be the same except for differences in the units of measurement. Standard techniques for the measurement of hydraulic conductivity on rock core are based on Darcy's law:

$$q = Q/A = -K\ (\Delta H/L), \quad (3)$$

where q = water flux (L/T),
Q = volumetric water flow rate (L^3/T),
A = cross-sectional area of core sample (L^2),
K = hydraulic conductivity (L/T),
ΔH = change in hydraulic head (L), and
L = core length (L).

Darcy's law is valid only for fluxes low enough to ensure that viscosity forces dominate within the pores and is assumed valid for the low fluxes measured in this study.

Combining equations 2 and 3 yields

$$k = - \frac{q\eta}{\rho g}, (L/\Delta H). \quad (4)$$

The units of k are those of area; however, k is often given in units of darcies or millidarcies (1 darcy = 9.87E-3 cm^2 for water at 25 °C). For the above equations, it is necessary to express L in centimeters, A in square centimeters, ΔH in atmospheres, Q in cubic centimeters per second, η in centipoises, and g in centimeters per second squared in order to obtain k in darcies.

Relative Permeability

Given an incompressible porous medium at constant temperature and pressure, factors such as fluid density and viscosity, porosity, and pore geometry can be considered constant under saturated conditions. However, in partially saturated media, pore-geometry factors and water-filled porosity change and k becomes a function of water content, when only the properties of the porous media are considered. This functional relation defines the relative permeability, k_r. As the water content of a sample decreases, its permeability also decreases as a function of the water potential (Richards, 1931). When the viscosity and density of the fluid are considered, the function is called unsaturated conductivity. Darcy's law usually is assumed to be valid for unsaturated flow conditions, but it may not apply at very low flow rates (Hillel, 1982). For a rock sample, Darcy's law can be written:

$$q = -K(\theta)\, dH/dL, \quad (5)$$

where θ = volumetric water content (cm^3/cm^3), and
$K(\theta)$ = hydraulic conductivity as a function of water content.

Water-Retention Curves

Another important rock matrix property is the water-retention function, $\psi(\theta)$, which expresses the dependence of matric potential (ψ) as a function of water content (θ). Matric potential, ψ, is a measure of the energy with which water is held in pores. Measurements of $\psi(\theta)$ are needed independently of $K(\theta)$ to predict water flow in transient conditions. As the water content of a porous medium decreases, water is removed from progressively smaller pores, and the water potential becomes more negative. At equilibrium, water content

is a function of the water potential. Water-retention curves obtained for desorption (drying) and sorption (wetting) conditions are not identical because of hysteresis effects. Hysteresis is attributed to: (1) The contact angle of the wetting fluid being greater during sorption than during desorption; (2) the geometric nonuniformity of pores (the "ink-bottle" effect, Hillel, 1982); and (3) entrapped air that decreases the water content of newly wetted media (Hillel, 1982). The water contents at various water potentials are a function of pore-size distribution and geometry, which are a function of texture, porosity, compaction, and structure (Hillel, 1982). The finer the texture, the greater the water retention at any particular potential, and the more gradual the slope of the curve. In a matrix containing a high fraction of large pores, once these pores are emptied, little water remains within the matrix.

METHODS OF MEASUREMENT FOR PHYSICAL PROPERTIES, PERMEABILITY, AND WATER RETENTION

Physical Property Measurements

Measurements of the static physical properties of the core samples were made. These measurements were used in the calculations and interpretations of the flow properties.

Porosity

Porosity was determined using air (or gas) pycnometry. Pycnometry is based on Boyle's gas law, $P_1 V_1 = P_2 V_2$, where the subscripts refer to initial (1) and final (2) pressure (P) and volume (V) of gas. In a closed sample chamber, the volume of gas in the system, V_2, after P_1 is increased to P_2, may be determined with and without a core sample in the chamber. The volume of solids and liquids in the sample is [V_2 (without sample) - V_2 (with sample)]. If this value is subtracted from the sample bulk volume, the result is the volume of gas-filled pores in the sample.

Bulk Density

Bulk density, ρ_b, is determined by measuring the weight and volume of a core sample. This is dependent on an accurate measurement of undisturbed sample volume.

The volume of the core is computed from measurements of size and shape. The core is ovendried and weighed. Then it is coated with a water-repellent substance, weighed in air, then submersed again. By using Archimedes' principle of volume displacement:

$$\rho_b = \frac{\text{ovendried weight of sample} \times \rho_w}{(\text{weight in air - weight in water})}, \qquad (6)$$

where ρ_w = the density of water.

The value of ρ_b computed by equation 6 is corrected for the weight and density of the water-repellent coating using the method described in Blake and Hartge (1986).

Grain Density

Grain (or particle) density, ρ_p, is measured with a water pycnometer (specific-gravity flask). A pycnometer is a glass flask fitted with a ground-glass stopper that is pierced lengthwise and has a capillary opening. A known weight of ovendried, crushed, or sieved media (maximum grain size <2 mm) is added to the flask and then weighed. Water then is added to the pycnometer, the stopper is inserted, and the flask is placed under a vacuum to extract all air from the pores. The flask is reweighed, then cleaned, filled with water only, and reweighed. Calculations are made using:

$$\rho_p = \frac{a \times \rho_w}{a - (b-c)}, \tag{7}$$

where a = weight of ovendried sample,
b = weight of pycnometer with sample and water, and
c = weight of pycnometer with water,

and corrections are made for temperature (ASTM, 1985).

The submersion method uses Archimedes' principle in which surface water is lightly wiped from a vacuum-saturated core sample, the sample is weighed in air, and then suspended from a scale and reweighed while submersed. The calculation of ρ_p is the same as that given in equation 6. In addition, any one of the three properties--grain density, bulk density, or porosity--can be calculated using equation 1 if the other two properties are known.

Intrinsic Permeability Measurements

Preliminary measurements of permeability were made using four different methods. These methods were: (1) Air permeability, (2) Klinkenberg permeability, (3) specific permeability to oil, and (4) specific permeability to water.

Air Permeability

Air permeability, k_a, is the coefficient governing convective transmission of air through a porous medium in response to a total pressure gradient (Hillel, 1982). This measurement can provide information on the effective sizes and the continuity of air-filled pores representing permeability with no fluid-matrix interactions. Air permeability is a simple, inexpensive method. Both constant-pressure (steady-state) and falling-pressure (nonsteady-state) measurement techniques commonly are used. Samples are prepared by extracting any hydrocarbons using cool toluene and leaching salts that may be present from using methyl alcohol. The samples then are dried in a humidity-controlled oven at 40- to 45-percent relative humidity and 60 °C until sample weights stabilize. Cores are placed in a rubber or latex collar, gas is forced through the core, and air permeability, k_a, is calculated using the following equation (Corey, 1986):

$$k_a = - \frac{(\eta_a)(q_a)(dx)}{d(p_a)}, \qquad (8)$$

where η_a = dynamic viscosity of air (M/LT),

q_a = volume flux per unit area measured (L^3/L^2T), and

dp_a/dx = measured air pressure gradient (M/T^2L).

Klinkenberg Permeability

Klinkenberg permeability measurements were performed to evaluate the effect of nonideal gas behavior on air permeability measurements. Air permeability for a dry medium is always larger than fluid permeability in water-saturated conditions. Klinkenberg (1941) reported differences in permeability between measurements using gas as the flowing fluid and using nonwetting fluids. These variations were attributed to gas slippage. This effect can be evaluated by measuring k_a (permeability of air) at a range of mean pressures and plotting gas permeability versus the reciprocal of the mean pressure, and extrapolating the reciprocal pressure to 0 to estimate permeability at infinite pressures. The value of k_a found by extrapolation equals the value of k obtained with liquids that do not wet the solid matrix.

Applying the slip theory to simple capillary models of porous media, Klinkenberg (1941) derived the following relation between the measured permeability and the mean pressure:

$$k_1 = k_a/(1+b/\bar{p}) = k_a - m\ (1/\bar{p}), \qquad (9)$$

where k_1 = permeability of the medium to a single liquid phase component filling the pores of the medium, computed,

k_a = permeability of the medium to a gas component filling the pores of the medium, measured,

$\bar{p}$ = mean flowing pressure of the gas at which k_g was measured,

$b = m/k_1$, which is a constant for a given gas in a given medium,

m = slope of the curve of k_a versus reciprocal mean pressure.

The constant, b, increases with decreasing permeability, k_a, as slippage effects become proportionally greater for smaller openings (Amyx and others, 1960). The term $b/\bar{p}$ is derived from the observation that the phenomenon of slip occurs when the diameter of a pore approaches the mean free path of the gas molecules, which is inversely proportional to the mean pressure, $\bar{p}$, at the surface of the sample. This method has the disadvantage of requiring many measurements to calculate a final permeability value, which is time consuming and causes additional expense.

Specific Permeability to Oil

Specific permeability to oil, also a nonwetting fluid, is used to interpolate between Klinkenberg permeability measurements and water. Oil is used because it does not have the polar properties of water. Cores were pressure saturated with a light mineral oil that has a dynamic viscosity of approximately 1.5 centipoise at ambient conditions (room temperature and atmospheric pressure). Fully saturated cores were placed into a hydrostatic core holder at an effective overburden pressure of 67 bars and specific permeability to oil was obtained in the same manner as air permeability. Measurements were made at a confining pressure of 67 bars, which is representative of the in-situ conditions within the formation prior to removal of core. This step is needed because consolidation of the core due to in-situ overburden pressure may cause as much as a 60-percent reduction in the specific permeability to oil (Amyx and others, 1960, p. 95).

Specific Permeability to Water

Specific permeability to water is used to determine permeability to the formation water. Cores were pressure saturated with a simulated formation water containing approximately 276 ppm (parts per million) total dissolved solids. The simulated formation water was prepared based on analyses of Calico Hills water samples and contained the following constituents:

Constituent	Grams per liter
NaCl	0.01
$MgCl_2 \cdot 6H_2O$	.01
Na_2SO_4	.04
$CaCl_2$	.04
$NaHCO_3$	.19
KCl	.01

The viscosity of water with this composition is approximately 0.98 centipoise at ambient conditions. This is 50 percent lower than the viscosity of the oil used in the measurement of specific permeability to oil. Cores were placed into a hydrostatic core holder that maintained an effective overburden pressure of 67 bars, and specific liquid permeability was determined.

Relative Permeability Measurements

There are four types of methods by which relative permeability data can be obtained:

1. Direct measurement in the laboratory by a steady-state, fluid flow process;
2. Measurement in the lab by displacement or nonsteady-state processes;
3. Estimations of relative permeability from water-retention curves; and
4. Inferences from field performance data.

In this data report, we discuss only the first two types.

Steady-State Methods

Steady-state methods all essentially depend on the same technique. A core sample is enclosed in lucite or a pressurized rubber sleeve, and a high flow rate and a large pressure differential is imposed across the core sample. Both ends of the sample are in contact with porous disks or test sections, or both, of materials similar to the sample to minimize capillary "end effects."

End effects refer to pressure gradients occurring at the ends of the sample because of the saturation discontinuity at the outflow face of the sample. At this face, all fluids are at the same pressure; yet, within the pores adjacent to the sample face, the saturation of the wetting phase approaches 100 percent. A saturation gradient, therefore, is established in the fluid phase within the sample. For a theoretical development of the principles that cause end effects, see Amyx and others (1960, p. 193). End effects either must be accounted for or minimized in all methods used.

The phases--gas-oil, oil-water, or gas-water--are injected simultaneously at the inlet end. Most tests start with saturated samples, which are desaturated during the measurement. The fluids are introduced at a particular ratio, and flow through the core is continued until the outflow ratio is equal to the injected ratio, thus, establishing steady-state conditions.

Percent saturation can be measured directly by core resistivity or tensiometry. Gravimetric measurements of percent saturation can be made by weighing the core, and volumetric methods require measuring all fluids injected into and produced from the sample.

Once saturation has been determined, the relative permeability can be calculated. The injected ratio is increased, removing more of the wetting phase, until steady-state conditions again are reached. The process is repeated until a complete curve is obtained. A resaturation curve can be obtained by using a core saturated with a nonwetting phase, which provides direct measurements of hysteretic effects. None of the data included in this report were generated using steady-state methods; however, steady-state methods will be compared at a later date.

Nonsteady-State Methods

A nonsteady-state method involves a sample in which only one fluid enters the sample and two fluids are discharged. Such methods include gas drive and centrifuge.

Gas-drive method

The sample is saturated with the wetting phase, and gas is injected at one end of the core. In order to reduce the data, three conditions must be met: (1) The flow rate must be high enough, and the pressure gradient across the sample large enough, to make capillary end effects negligible; (2) the gas-saturation-pressure drop must be linear; and (3) the flow must be horizontal, the core must be small, and the test time short enough to prevent gravitational redistribution of fluid within the core. Gas injected and liquid produced over time are measured with pressures at inlet and outlet constant, as indicated in the following equation:

$$G = \frac{2\ G_i\ P_i}{V_p\ (P_i + P_o)}, \tag{10}$$

where G = cumulative injected gas as pore volume (cm^3/cm^3),
G_i = cumulative injected gas at inlet pressure (cm^3),
V_p = total pore volume of sample (cm^3),
P_i = inlet pressure ($dynes/cm^2$), and
P_o = outlet pressure ($dynes/cm^2$).

Cumulative fluid produced is plotted against fluid produced in pore volume. The slope of a fitted line represents the fraction of the total outflow volume from the sample that is liquid at any given time, which defines the following:

$$f = d(S_a)/dG, \tag{11}$$

where f = the fractions of the total outflow that is fluid, and
$d(S_a)/dG$ = the slope of the line of gas saturation.

The air-to-water permeability ratio, or relative permeability of gas, k_a, to fluid, k_w, can be calculated:

$$\frac{k_a}{k_w} = \frac{1-f}{f(\eta_a/\eta_w)}, \tag{12}$$

where η_a and η_w = viscosity values of the gas and fluid (water).

This particular value of the ratio applies at the gas saturation at the outflow face. Gas saturation at the outflow face, o, is:

$$(S_a)_o = S_a - Gf. \tag{13}$$

Thus, relative permeability ratios are obtained as a function of saturation. Actual values of relative permeability require that one of the phases be measured for a saturated permeability value. The detailed calculations are discussed in Amyx and others (1960, p. 190).

In comparison with steady-state methods described above, the gas-drive method uses considerably less apparatus, is very simple, and can be performed rapidly on small core samples. A disadvantage is that it cannot determine relative permeability ratios at low values of gas saturation. End effects are not important due to the high pressure gradients created across the core sample (Owens and others, 1956).

Centrifuge method

Relative permeability can be determined by a transient outflow centrifuge method (Hagoort, 1980; Van Spronsen, 1982). An advantage of this method is the ability to obtain values at low gas saturations. First, cores are pressure saturated with the simulated formation water. The core then is placed into a centrifuge and spun at 11,750 rpm. The quantity of fluid produced versus time is monitored continuously for approximately 275,000 seconds. The production of fluid as a function of time usually is measured by taking photographs of a transparent graduated collection tube using stroboscopic illumination. The volume of water for each sample is used to calculate the values of unsaturated hydraulic conductivity. These values then are converted to relative permeability by inverting equation 2, thereby taking into account the viscosity and density of the formation water and acceleration of gravity. Example calculations are shown in the section on measuring water-retention curves with a centrifuge.

The capillary end effects can be minimized by using a high centrifugal acceleration; the centrifugal force on the liquid phases still will be small compared with the capillary forces on a pore scale. If the centrifugal forces on a pore scale become important, the end points and the shape of the relative permeability curve change (Van Spronsen, 1982).

The advantage of the centrifugal method is that it works independently of matric potential gradients. This can be important for unsaturated porous media or rocks where matric potential gradients can cause gradients of water content and conductivity, thus, introducing an often undesirable complexity (Nimmo and others, 1987).

Methods also have been developed to measure unsaturated conductivity using steady-state outflow of water from an unsaturated sample spinning in a centrifuge (Nimmo and others, 1987; Conca and Lane, 1988).

Water-Retention Measurements

The quantity of water remaining in a porous medium at a specified water content is a function of the sizes and volumes of the water-filled pores and, hence, is a function of the matric potential. Water-retention relations, expressing the dependence of saturation on matric potential, are needed to establish a known matric potential for each core sample matrix of interest.

Porous Plate Methods

Several methods involve using a porous plate, a type of membrane through which water but not air will flow owing to pressure or vacuum. Such methods include vacuum, pressure extractor, and submersible-pressure-outflow cell. Porous plates usually are made of ceramic materials with pore-size distributions selected to retain water over various pressure or vacuum ranges. The smaller the pores, the higher the pressure required, and the longer it takes to reach matric potential equilibrium.

Vacuum

In the vacuum method, a water-saturated core sample is placed in contact with a water-saturated porous plate to establish a continuous water column. The upper end of the sample is at atmospheric pressure. A pressure differential can be created across the core sample and controlled by applying a vacuum at the bottom of the porous plate by using a vacuum pump or a hanging water column. The pressure differential forces water out of the sample until a known pressure is established, which, at equilibrium, is the matric potential, ψ, in the sample. The water released from the sample is measured, or the sample is weighed to determine water content, θ. The disadvantage of this method is that the lower value of matric potential is limited to about -0.8 bar (Klute, 1986).

Pressure extractor

In a pressure extractor, the sample is placed on a porous plate with a sheet-rubber backing. An outlet through the plate keeps the bottom of the plate and bulk water at atmospheric pressure. The range of matric potential for pressure plates is determined by the safe working pressure of the chamber and the pressure differential at which air will bubble through the pores in the plate. Once water is pushed out of the saturated samples and allowed to equilibrate at a given pressure, the samples are removed from the chamber and gravimetric water content is determined. Samples and plates are resaturated to determine additional $\psi(\theta)$ points in order to construct the water-retention curve. Disadvantages of this method include problems with determining when equilibrium is established. There also are problems because of changes in core water potential when pressure is released from the extractor as a result of backflow of water into the core from the plate or as a result of production of air bubbles in the core, or both, causing redistribution of water into larger size pores (Klute, 1986).

Submersible-pressurized-outflow cell

A porous plate method that helps to solve some of these problems is the submersible-pressurized-outflow cell (SPOC) (Constantz and Herkelrath, 1984). This method encloses a single sample on a porous plate in a cell with a pressure inflow port on top connected to a quick-release compression fitting. Water outflow is through the bottom of the plate. The cell is then suspended in a constant-temperature water bath and pressure is applied to remove water from the sample. The entire cell is weighed, suspended in water, while hanging from the bottom of a scale. The difference in weights is equal to the quantity of water lost. Equilibrium can be determined by cessation of water loss, and samples are weighed without pressure loss eliminating backflow and bubble formations. Sorption measurements, which are complicated by the presence of air under the plate in a pressure extractor that tends to break the continuous water columns, are easily accomplished in a SPOC because water flows directly into the sample through the porous plate that is in contact at all times with the water in the bath.

Centrifugation

Saturated core samples are placed on a permeable, wet membrane and located in a holder in a centrifuge rotor. The water is expelled from the core at increasing rates of rotation and is viewed in a chamber in the holder below the core through a port with a stroboscope during centrifuge action. It is essential to take readings of expelled water volume during rotation and to increase the rate of rotation without any decrease, in order to prevent redistribution of the fluid in the sample. The volume of water remaining in the sample then is divided by the total pore volume of the samples. Calculations of the water-retention curve are as follows:

1. The extracted volume reading, V (at each angular velocity) is converted to average saturation for the core, S_c, using the total pore volume of the core, V_{tot}, by:

$$S_c = 1 - (V/V_{tot}). \tag{14}$$

2. Angular velocity, ω, is converted to pressure, P, by:

$$P = [(\rho_w - \rho_g)\omega^2/2] \cdot (re^2 - r^2), \tag{15}$$

where ρ_w = density of water (g/cm),
ρ_g = density of gas (g/cm),
ω = angular velocity (radians/second),
r = distance from the center of rotation (cm), and
r_e = radius of the core bottom (cm), calculated as

$$\omega(\text{rad/sec}) = \text{RPM} \cdot \frac{2\pi(\text{rad/rev})}{60(\text{sec/min})}. \tag{16}$$

3. PS_c is plotted against P. Assuming capillary pressure is equal to P, then the water-retention curve can be generated from this plot.

4. The water-retention curve is derived from the curve in step 3 using:

$$\psi(\theta) = \frac{d(PS\text{-}c)}{dP}. \tag{17}$$

Good agreement between centrifugation and porous plate methods has been found by Slobod and others (1951) and by Hoffman (1963). The porous plate method may require weeks, whereas the centrifuge method may require only a few days to complete. The centrifuge generally is nondestructive and provides reproducible results. Both desorption and sorption curves can be produced (Skuse, 1984).

Mercury Intrusion Porosimetry

Because mercury is a nonwetting liquid, it will not enter pores by capillary action. Mercury can, however, be forced into pores by intruding it under the application of external pressure. The size of the pores that are intruded is inversely proportional to the applied pressure (ASTM, 1985):

$$d = (4\gamma\,|\cos\alpha|)/P, \tag{18}$$

where d = diameter of the pore (cm),
γ = surface tension of mercury (dynes/cm^2),
α = contact angle of mercury with the surface of the porous media (°), and
P = absolute pressure (dynes/cm^2).

The volume of mercury injected at each pressure determines the nonwetting-phase saturation. This is a very fast method that was developed to accelerate the process of water-retention determination. Disadvantages of this method are (1) the difference in wetting properties between mercury and water, and (2) the permanent loss of the core sample (Amyx and others, 1960).

Amyx and others (1960) claim that the porous plate method is superior to other methods because it is closer to simulating actual wetting conditions and, hence, is used as a standard method for comparison. This idea may have merit for several reasons. The contact angle for mercury against rock surfaces is 140°, while that of water is approximately 0°, and the ratio of mercury capillary pressure to water-air capillary pressure is about 5 (Amyx and others, 1960). Purcell (1949) showed graphically that the agreement of data between the two methods is good when corrected by this ratio. However, a question exists as to whether the contact angle can be used as the only basis of the pressure ratio [as used in mercury porosimetry standard methods in ASTM (1985)]. The mean curvature of an interface in rock is a unique function of fluid saturation defining the pressure ratio as 6.57 rather than 5 (Amyx and others, 1960). Brown (1951) reported the correlating factor between the two methods to be a function of the porous medium and defined the ratio as 7.5 for sandstone or 5.8 for limestone. Therefore, uncertainty about the value of the correlating factor between mercury and water wetting properties introduces doubt regarding the accuracy of the method.

RESULTS OF PHYSICAL PROPERTY, PERMEABILITY, AND WATER-RETENTION MEASUREMENTS

The methods described were used to measure properties of 73 rock core samples. There were both vertically and horizontally oriented samples from many of the borehole depth intervals.

Core Physical Properties

Measured values of porosity, grain density, and bulk density for core samples are summarized in table 2. Measurements for each property were made at the U.S. Geological Survey petrophysics laboratory in Golden, Colo. (USGS-P); or at Core Laboratories, Inc., in Aurora, Colo. (CLI), or both. USGS-P used both Archimedes' principle and air pycnometry to measure porosity and grain density, while CLI used only helium pycnometry. Bulk density was measured by USGS-P using Archimedes' principle and the caliper measurement technique.

Intrinsic Permeability

Measured values for saturated permeability using the air permeability method and three types of liquid permeability methods are listed in table 3. Air permeability values were obtained using helium pycnometry. Permeability to specific liquid was measured using the simulated formation water method (detailed in the "Methods" section) and hence referred to as specific permeability to water. The entry "0.00" indicates that the permeability was <0.01 millidarcies (mD). It was suggested by CLI that sample 2U may have developed a fracture during testing and the measurement values may be considered invalid. It also may be possible that the entire original section of core from which the samples came may have been fractured. For this reason, data from 2U, 2UH, and 2UP were not used in analyses of permeability.

Relative Permeability and Unsaturated Hydraulic Conductivity

Relative permeability and the corresponding calculated unsaturated hydraulic-conductivity values are listed in table 4 for 10 samples; 9 samples were analysed using the centrifuge method; and 3 of these 9 samples, plus an additional sample, were analyzed using the gas-drive method. The conversions for the unsaturated hydraulic conductivity calculations are as follows:

Saturated hydraulic conductivity (cm/s) = saturated permeability (mD) $\times$ 980 (cm/s) $\times$ 9.87 $\times$ 10^{-12}/0.01002 (poise); unsaturated hydraulic conductivity (cm/s) = [saturated permeability (mD) $\times$ relative permeability fraction] $\times$ 9.87 $\times$ 10^{-12} $\times$ 980 (cm/s)/0.01002 (poise). Related graphical representations are shown in appendix I.

Water-Retention Curves

Water retention, or matric potential versus water content, is listed in tables 5 and 6. Volumetric water content at various matric potentials for 11 core samples is listed in table 5. All tests were run by CLI. Porous plate (pressure plate) values were obtained using a *pressure extractor*. Water-retention values listed in table 6 were obtained by USGS-P using *mercury intrusion porosimetry* on nine vertical core samples. Related graphical representations of water-retention data are shown in appendix II.

Table 2.--*Physical properties of core samples: Porosity, grain density, and bulk density*

[All porosity and grain density measured by gas pycnometry unless otherwise noted; A, value obtained by Archimedes' principle; M, volume of sample measured by caliper and calculated; cm^3/cm^3, cubic centimeter per cubic centimeter; g/cm^3, grams per cubic centimeter; --, no data]

Sample label	Porosity (cm^3/cm^3)	Grain density (g/cm^3)	Bulk density (g/cm^3)
1U	0.363	2.30	--
	.364	2.30	
1UH	.387	2.30	--
	.391	2.32	
2U	.351	2.29	--
	.354	2.30	
2UH	.381	2.24	--
1P	.145	2.30	--
	.149	2.30	
1PH	.141	2.31	--
2P	.227	2.25	--
	.231	2.25	
2PH	.266	2.25	--
3P	.362	2.32	--
	.335	2.30	
	.336	2.31	
3PH	.347	2.30	--
20A	.212	2.29	--
	.228	2.21	
20AP	.260 A	2.29 A	1.69 A
			1.71 M
12A	.271	2.29	--
12AP	.309 A	2.38 A	1.64 A
			1.65 M
13A	.333	2.29	--
13AP	.334 A	2.35 A	1.56 A
			1.58 M
14A	.324	2.29	--
14AP	.349 A	2.21 A	1.44 A
			1.44 M
16A	.364	2.23	--
16AP	.333 A	2.23 A	1.49 A
			1.49 M
15A	.284	2.28	--
15AP	.266 A	2.24 A	1.65 A
			1.65 M
17A	.304	2.34	--
	.266	2.31	
	.280	2.26	
17AH	.276	2.25	--
17AP	.274 A	2.29 A	1.66 A
			1.67 M

Table 2.--*Physical properties of core samples: Porosity, grain density, and bulk density*--Continued

Sample label	Porosity (cm^3/cm^3)	Grain density (g/cm^3)	Bulk density (g/cm^3)
18A	0.278	2.30	--
	.248	2.28	
18AH	.236	2.29	--
18AP	.275 A	2.32 A	1.68 A
			1.70 M
19A	.363	2.35	--
	.272	2.25	
19AH	.283	2.22	--
19AP	.327 A	2.32 A	1.56 A
			1.57 M
8A	.299	2.26	--
8AP	.331 A	2.32 A	1.55 A
			1.57 M
11A	.313	2.32	--
11AP	.326 A	2.33 A	1.57 A
			1.58 M
1A	.228	2.61	--
1AP	.277	2.58 A	1.87 M
7AP	.287 A	2.27 A	1.62 A
	.254	2.27 A	1.63 M
9A	.285	2.35	--
	.282	2.32	
9AH	.271	2.31	--
9AP	.297 A	2.35 A	1.66 A
	.274	2.29	1.67 M
10A	.316	2.42	--
	.311 A	2.36 A	1.62 A
	.291	2.31	1.64 M
4AP	.431 A	2.41 A	1.37 A
	.423	2.40	1.38 M
5A	.414	2.34	--
	.416	2.33	
	.427	2.36	
5AP	.440 A	2.36 A	1.33 A
	.441	2.33	1.30 M
2A	.510	2.34	--
	.490	2.33	
	.473	2.31	
	.485	2.34	
2AP	.504 A	2.35 A	1.17 A
	.502	2.34	1.16 M

Table 2.--*Physical properties of core samples: Porosity, grain density, and bulk density*--Continued

Sample label	Porosity (cm^3/cm^3)	Grain density (g/cm^3)	Bulk density (g/cm^3)
6A	0.364	2.33	--
		2.35	
6AP	.437 A	2.30 A	1.30 A
	.454	2.32	1.26 M
3A	.443	2.33	--
	.441	2.34	
	.443	2.34	
3AH	.440	2.33	--
3AP	.440 A	2.33 A	1.31 A
	.454	2.32	1.27 M
1V	.436	2.44	--
	.405	2.32	
1VP	.419 A	2.34 A	1.36 A
	.418	2.32	1.35 M
5-2	.321	2.28	--
	.311	2.26	
	.326	2.29	
5-2H	.320	2.25	--
5-1B	.423	2.33	--
4-4	.399	2.37	--
	.408	2.40	
4-4H	.412	2.36	--
4-5	.472	2.37	--
	.482	2.40	
4-5H	.470	2.35	--
5-6	.464	2.25	--
5-7	.455	2.34	--
4-6	.281	2.28	--
	.287	2.29	
4-6H	.336	2.24	--
4-7	.355	2.27	--
	.362	2.29	
4-7H	.408	2.42	--
5-1	.396	2.31	--
5-1A	.411	2.35	--
5-8	.345	2.33	--
5-9	.287	2.26	--
	.308	2.23	
	.289	2.25	

Table 3.--*Intrinsic permeability values for core samples*

[All values in millidarcies; --, no data]

Sample label	Air permeability	Klinkenberg permeability	Specific permeability to nonpolar oil	Specific permeability to water
1U	0.17	0.24	--	0.01
	.07			1.10
	2.80			1.30
1UH	1.20	.26	0.35	.22
			.25	.27
2U	.35	30.50	--	.01
	.29			1.70
	68.00			47.00
2UH	46.00	--	--	--
2UP	--	.35	37.00	9.90
1P	.00	.00	--	.00
	.02			.00
	.01			
1PH	.00	--	--	--
2P	.22	.03	--	.03
	.18	.04		.04
	.09			.03
2PH	.30	.05	.02	.01
3P	.26	.02	--	.01
	.36	.02		.04
	.53			.05
	.20			
3PH	.25	.20	.05	.03
20A	.02	.03	--	.00
	.47			.00
20AP	--	--	--	.07
12A	.18	.04	--	.00
12AP	--	--	--	.02
13A	.10	.02	--	.00
13AP	--	--	--	.02
14A	.22	.01	--	.01
14AP	--	--	--	.03
16A	.20	.02	--	.02
16AP	--	--	--	.03
15A	.18	--	--	.01
15AP	--	--	--	.02

Table 3.--*Intrinsic permeability values for core samples*--Continued

Sample label	Air permeability	Klinkenberg permeability	Specific permeability to nonpolar oil	Specific permeability to water
17A	0.06		--	0.01
	.17	0.03		
	.08			
17AH	.09	.02	0.01	.01
17AP	--	--	--	.02
18A	.03	.03	--	.00
	.07			
18AH	.01	.01	.00	.01
				.00
18AP	--	--	--	.006
19A	.19	--	--	.00
	.14	.05		.00
19AH	.28	.04	.02	.01
			.07	
19AP	--	--	--	.02
8A	.07	--	.00	.00
11A	.06	.02	--	.00
11AP	--	--	--	.02
1A	.23	.04	--	.00
7AP	--	--	--	.06
9A	.05	.01	--	.00
				.00
9AH	.04	.01	.00	--
9AP	--	--	--	.00
				.00
10A	.09	.02	.00	.00
	.12	.01		
		.05		
10AP	--	--	--	.01
				.005
4AP	--	--	--	.02
				.00
5A	132.00	--	--	41.00
	142.00			100.00
5AP	129.00	--	--	159.00
2A	290.00	--	--	64.00
	264.00			198.00
	368.00			192.50
	374.00			129.50

Table 3.--*Intrinsic permeability values for core samples*--Continued

Sample label	Air permeability	Klinkenberg permeability	Specific permeability to nonpolar oil	Specific permeability to water
6A	--	--	--	242.40
3A	267.00	--	--	90.00
	247.00			195.00
3AH	293.00	312.00	282.00	--
	315.00			
3AP	--	--	--	220.00
				287.50
IV	30.00	22.00	--	14.00
	34.00			17.00
IVP	--	--	--	19.20
5-2	5.50	3.21	--	2.10
	5.30			
	5.20			
5-2H	9.50	9.16	6.90	3.30
5-1B	117.00	90.00	--	.76
4-4	2.30	1.26	--	.86
4-4H	4.80	3.52	3.40	1.90
4-5	90.00	33.00	--	20.00
	92.00	89.00		51.00
	93.00			
4-5H	111.00	111.30	94.00	74.00
5-6	35.00	33.00	--	20.00
5-7	32.00	29.00	--	.69
4-6	53.00	58.00	--	29.00
	78.00			
	152.00			
4-6H	29.00	23.40	19.00	8.70
4-7	21.00	21.00	--	.46
	17.00			
4-7H	27.00	3.00	--	2.20
5-1	42.00	43.00	--	14.00
	45.00			
5-1H	--	--	--	2.20
5-1A	247.00	210.00	--	.67
5-8	2.40	.60	--	.46
5-9	223.00	308.00	--	140.00
	362.00			184.00
	350.00			

Table 4.--*Relative permeability and corresponding calculated unsaturated hydraulic-conductivity values*

[mD, millidarcies; cm/s, centimeter per second; relative permeability (fraction), relative permeability to water, fraction]

Sample label	Hydraulic conductivity saturated (cm/s)	Permeability saturated (mD)	Percent saturation	Relative permeability (fraction)	Hydraulic conductivity unsaturated (cm/s)
			GAS-DRIVE METHOD RESULTS		
5-2	5.31×10^{-6}	5.5	100.0	1.0	5.31×10^{-6}
			88.8	.124	6.58×10^{-7}
			87.0	.088	4.67×10^{-7}
			85.9	.069	3.66×10^{-7}
			84.9	.056	2.97×10^{-7}
			82.7	.033	1.75×10^{-7}
			80.7	.019	1.01×10^{-7}
			79.0	.013	6.90×10^{-8}
			77.7	.0084	4.46×10^{-8}
			76.4	.0050	2.65×10^{-8}
			74.7	.0035	1.86×10^{-8}
			73.2	.0019	1.01×10^{-8}
			71.8	.00078	4.14×10^{-9}
			70.9	.00039	2.07×10^{-9}
3P	2.90×10^{-8}	.03	100.0	1.0	2.90×10^{-8}
			87.8	.541	1.57×10^{-8}
			83.7	.421	1.22×10^{-8}
			78.7	.300	8.69×10^{-9}
			72.3	.162	4.69×10^{-9}
			68.4	.097	2.81×10^{-9}
			65.6	.063	1.82×10^{-9}
			63.2	.040	1.16×10^{-9}
			61.4	.026	7.53×10^{-10}
			59.9	.017	4.92×10^{-10}
			58.3	.0097	2.81×10^{-10}
			57.2	.0057	1.65×10^{-10}
			56.4	.0036	1.04×10^{-10}
IV	1.75×10^{-5}	18.1	100.0	1.0	1.75×10^{-5}
			89.4	.075	1.31×10^{-6}
			88.1	.052	9.09×10^{-7}
			87.4	.043	7.51×10^{-7}
			86.8	.037	6.46×10^{-7}
			86.2	.031	5.42×10^{-7}
			84.8	.019	3.32×10^{-7}
			83.5	.012	2.10×10^{-7}
			82.7	.0088	1.54×10^{-7}
			81.5	.0062	1.08×10^{-7}
			79.3	.0022	3.84×10^{-8}
			78.4	.0015	2.62×10^{-8}
			76.9	.00066	1.15×10^{-8}
			76.1	.00038	6.64×10^{-9}

Table 4.--*Relative permeability and corresponding calculated unsaturated hydraulic-conductivity values*--Continued

Sample label	Hydraulic conductivity saturated (cm/s)	Permeability saturated (mD)	Percent saturation	Relative permeability (fraction)	Hydraulic conductivity unsaturated (cm/s)
			GAS-DRIVE METHOD RESULTS--Continued		
1U	9.65×10^{-9}	0.01	100.0	1.0	9.65×10^{-9}
			76.7	.172	1.66×10^{-9}
			74.2	.137	1.32×10^{-9}
			72.5	.121	1.17×10^{-9}
			67.1	.070	6.76×10^{-10}
			63.6	.037	3.57×10^{-10}
			62.0	.029	2.80×10^{-10}
			59.0	.017	1.64×10^{-10}
			57.1	.010	9.65×10^{-11}
			56.0	.008	7.72×10^{-11}
			52.8	.0036	3.48×10^{-11}
			51.3	.0014	1.35×10^{-11}
			CENTRIFUGE METHOD RESULTS		
	5.31×10^{-6}	5.5	100.0	1.0	5.31×10^{-6}
			72.0	.034	1.81×10^{-7}
			71.8	.033	1.75×10^{-7}
			70.5	.024	1.27×10^{-7}
			68.2	.020	1.06×10^{-7}
			65.5	.010	5.31×10^{-8}
			63.0	.0061	3.24×10^{-8}
			59.9	.0034	1.81×10^{-8}
			58.6	.0027	1.43×10^{-8}
			57.2	.0017	9.03×10^{-9}
			56.0	.0014	7.43×10^{-9}
			52.6	.00066	3.50×10^{-9}
			51.1	.00038	2.02×10^{-9}
			50.4	.00034	1.81×10^{-9}
			46.3	.00016	8.49×10^{-10}
			44.2	.000082	4.35×10^{-10}
			43.1	.000067	3.56×10^{-10}
			42.9	.000061	3.24×10^{-10}
			41.7	.000053	2.81×10^{-10}
			39.4	.000028	1.49×10^{-10}

Table 4.--*Relative permeability and corresponding calculated unsaturated hydraulic-conductivity values*--Continued

Sample label	Hydraulic conductivity saturated (cm/s)	Permeability saturated (mD)	Percent saturation	Relative permeability (fraction)	Hydraulic conductivity unsaturated (cm/s)
			CENTRIFUGE METHOD RESULTS--Continued		
2A	1.46×10^{-4}	151.5	100.0	1.0	1.46×10^{-4}
			86.0	.053	7.75×10^{-6}
			85.0	.046	6.73×10^{-6}
			83.6	.033	4.83×10^{-6}
			82.6	.024	3.51×10^{-6}
			81.5	.017	2.49×10^{-6}
			80.7	.014	2.05×10^{-6}
			79.5	.010	1.46×10^{-6}
			78.0	.0064	9.36×10^{-7}
			77.0	.0049	7.17×10^{-7}
			75.7	.0034	4.97×10^{-7}
			74.2	.0021	3.07×10^{-7}
			72.9	.0012	1.75×10^{-7}
			71.8	.00068	9.94×10^{-8}
			71.0	.00040	5.85×10^{-8}
			70.2	.00021	3.07×10^{-8}
			69.5	.000072	1.05×10^{-8}
18A	2.90×10^{-9}	.003	100.0	1.0	2.90×10^{-9}
			97.3	.305	8.83×10^{-10}
			96.4	.222	6.43×10^{-10}
			95.3	.129	3.74×10^{-10}
			94.3	.079	2.29×10^{-10}
			93.1	.031	8.98×10^{-11}
			92.1	.011	3.19×10^{-11}
			91.7	.0014	4.05×10^{-12}
4-5H	7.14×10^{-5}	74	100.0	1.0	7.14×10^{-5}
			64.1	.039	2.79×10^{-6}
			62.4	.032	2.29×10^{-6}
			59.0	.019	1.36×10^{-6}
			57.5	.014	1.00×10^{-6}
			57.1	.013	9.29×10^{-7}
			51.9	.0045	3.21×10^{-7}
			50.5	.0031	2.21×10^{-7}
			49.9	.0024	1.71×10^{-7}
			49.0	.0020	1.43×10^{-7}
			48.3	.0014	1.00×10^{-7}

Table 4.--*Relative permeability and corresponding calculated unsaturated hydraulic-conductivity values*--Continued

Sample label	Hydraulic conductivity saturated (cm/s)	Permeability saturated (mD)	Percent saturation	Relative permeability (fraction)	Hydraulic conductivity unsaturated (cm/s)
			CENTRIFUGE METHOD RESULTS--Continued		
17A	1.45×10^{-8}	0.015	100.0	1.0	1.45×10^{-8}
			95.8	.578	8.37×10^{-9}
			94.3	.506	7.33×10^{-9}
			92.3	.377	5.46×10^{-9}
			90.0	.297	4.30×10^{-9}
			88.4	.221	3.20×10^{-9}
			85.3	.157	2.27×10^{-9}
			80.2	.034	4.92×10^{-10}
			80.0	.030	4.34×10^{-10}
			78.8	.020	2.90×10^{-10}
			77.0	.0061	8.83×10^{-11}
			76.1	.0022	3.19×10^{-11}
			75.7	.00028	4.05×10^{-12}
5-9	1.78×10^{-5}	184	100.0	1.0	1.78×10^{-5}
			76.9	.026	4.62×10^{-7}
			72.5	.0097	1.72×10^{-7}
			71.5	.0081	1.44×10^{-7}
			68.9	.0053	9.41×10^{-8}
			67.5	.0034	6.04×10^{-8}
			65.8	.0028	4.97×10^{-8}
			63.4	.0014	2.49×10^{-8}
			61.3	.0010	1.78×10^{-8}
			60.1	.00047	8.35×10^{-9}
			59.1	.00042	7.46×10^{-9}
			55.8	.00013	2.31×10^{-9}
			50.9	.0000077	1.37×10^{-10}
1UH	2.12×10^{-7}	.22	100.0	1.0	2.12×10^{-7}
			81.4	.338	7.18×10^{-8}
			78.9	.292	6.20×10^{-8}
			74.7	.218	4.63×10^{-8}
			70.8	.164	3.48×10^{-8}
			65.1	.099	2.10×10^{-8}
			63.2	.077	1.64×10^{-8}
			60.1	.057	1.21×10^{-8}
			58.4	.044	9.34×10^{-9}
			54.2	.029	6.16×10^{-9}
			51.6	.016	3.40×10^{-9}
			47.8	.0094	2.00×10^{-9}
			45.9	.0049	1.04×10^{-9}
			43.6	.0035	7.43×10^{-10}

Table 4.--*Relative permeability and corresponding calculated unsaturated hydraulic-conductivity values*--Continued

Sample label	Hydraulic conductivity saturated (cm/s)	Permeability saturated (mD)	Percent saturation	Relative permeability (fraction)	Hydraulic conductivity unsaturated (cm/s)
			CENTRIFUGE METHOD RESULTS--Continued		
1UH--Continued			39.7	0.0014	2.97×10^{-10}
			38.0	.00063	1.34×10^{-10}
			37.3	.00056	1.19×10^{-10}
			34.8	.00023	4.88×10^{-11}
			34.7	.00021	4.46×10^{-11}
			33.8	.00018	3.82×10^{-11}
			30.8	.000027	5.73×10^{-12}
4-6H	8.40×10^{-6}	8.7	100.0	1.0	8.40×10^{-6}
			81.8	.061	5.12×10^{-7}
			81.2	.057	4.79×10^{-7}
			80.3	.047	3.95×10^{-7}
			78.3	.034	2.86×10^{-7}
			76.5	.020	1.68×10^{-7}
			75.3	.017	1.43×10^{-7}
			74.5	.013	1.09×10^{-7}
			73.9	.012	1.01×10^{-7}
			72.3	.0079	6.63×10^{-8}
			71.6	.0067	5.63×10^{-8}
			70.0	.0044	3.70×10^{-8}
			69.4	.0033	2.77×10^{-8}
			66.9	.0017	1.43×10^{-8}
			65.7	.0014	1.18×10^{-8}
			64.7	.00094	7.89×10^{-9}
			63.7	.00810	6.80×10^{-9}
			62.4	.00047	3.95×10^{-9}
			62.0	.00045	3.78×10^{-9}
			61.9	.00033	2.77×10^{-9}
			61.3	.00031	2.60×10^{-9}
			57.8	.000096	8.06×10^{-10}
			57.3	.000066	5.54×10^{-10}
			56.7	.000050	4.20×10^{-10}
			55.3	.000019	1.60×10^{-10}

Table 4.--*Relative permeability and corresponding calculated unsaturated hydraulic-conductivity values*--Continued

Sample label	Hydraulic conductivity saturated (cm/s)	Permeability saturated (mD)	Percent saturation	Relative permeability (fraction)	Hydraulic conductivity unsaturated (cm/s)
			CENTRIFUGE METHOD RESULTS--Continued		
IV	1.75×10^{-5}	18.1	100.0	1.0	1.75×10^{-5}
			95.3	.308	5.38×10^{-6}
			93.8	.230	4.02×10^{-6}
			92.4	.193	3.37×10^{-6}
			90.5	.126	2.20×10^{-6}
			88.7	.093	1.62×10^{-6}
			86.6	.046	8.04×10^{-7}
			85.8	.039	6.81×10^{-7}
			85.1	.028	4.89×10^{-7}
			83.8	.021	3.67×10^{-7}
			81.9	.0057	9.96×10^{-8}
			81.1	.0045	7.86×10^{-8}
			80.2	.0022	3.84×10^{-8}
			79.3	.0010	1.75×10^{-8}
3P	2.90×10^{-8}	.03	100.0	1.0	2.90×10^{-8}
			88.5	.588	1.71×10^{-8}
			88.1	.582	1.69×10^{-8}
			84.5	.443	1.28×10^{-8}
			78.2	.248	7.19×10^{-9}
			75.2	.156	4.52×10^{-9}
			74.8	.152	4.41×10^{-9}
			70.2	.096	2.78×10^{-9}
			66.6	.047	1.36×10^{-9}
			63.7	.033	9.57×10^{-10}
			60.1	.014	4.06×10^{-10}
			58.5	.0078	2.26×10^{-10}
			57.2	.0055	1.60×10^{-10}
			54.5	.0016	4.64×10^{-11}

Table 5.--*Water retention for pressure plate and*

[Water retention, in percent volumetric water content; matric

Sample label	Method	Matric								
		0.03	0.07	0.14	0.28	0.34	0.55	0.69	1.03	1.38
IV	PLATE	0.93	0.91	0.86	0.76	--	0.66	--	0.57	--
	CENT.	--	.95	.87	--	0.75	--	0.68	--	0.61
	CENT.	--	1.00	.98	--	.81	--	.69	--	--
2A	PLATE	--	1.00	.86	.67	--	.63	--	.60	--
	CENT.	--	.91	.77	--	.65	--	.53	--	.41
4-5	PLATE	--	.98	.98	.94	--	.61	--	.50	--
	CENT.	--	1.00	1.00	--	.58	--	.40	--	.30
4-5H	CENT.	--	1.00	.90	--	.60	--	.38	--	.28
4-6	PLATE	--	1.00	1.00	.97	--	.94	--	.91	--
	CENT.	--	1.00	1.00	--	.97	--	.92	--	.86
4-6H	CENT.	--	1.00	1.00	--	.76	--	.68	--	.60
4-7	PLATE	--	.97	.92	.82	--	.71	--	.67	--
	CENT.	--	.94	.78	--	.69	--	.63	--	.55
4-7H	PLATE	.96	.95	.91	.79	--	.59	--	.50	--
5-9	PLATE	--	.83	.74	.62	--	.58	--	.55	--
	CENT.	--	.95	.87	--	.63	--	.53	--	.45
1U	PLATE	--	--	--	--	--	--	.78	--	.68
	CENT.	--	1.00	1.00	--	1.00	--	.98	--	--
1UH	PLATE	.98	.98	.96	.83	--	.71	--	.63	--
	CENT.	--	1.00	1.00	--	.84	--	.70	--	.63
5-2	CENT.	--	1.00	1.00	--	.91	--	.84	--	.75
	PLATE	--	--	--	--	--	--	.59	--	.47
	CENT.	--	--	--	--	--	--	1.00	--	--
17A	CENT.	--	1.00	1.00	--	1.00	--	.98	--	.97
	CENT.	--	--	--	--	--	--	1.00	--	--
	PLATE	--	--	--	--	--	--	.91	--	.85
18A	CENT.	--	--	--	--	--	--	1.00	--	--
	PLATE	--	--	--	--	--	--	.98	--	.93
3P	CENT.	--	--	--	--	--	--	1.00	--	--
	PLATE	--	--	--	--	--	--	.91	--	.78

centrifuge methods on vertical and horizontal core samples

potential in bars; PLATE, pressure plate; CENT., centriufge; --, no data]

potential										
1.72	2.41	2.76	3.45	4.14	5.52	6.90	8.28	13.79	34.48	68.97
--	0.47	--	--	--	--	0.41	--	--	--	--
--	--	0.55	--	0.51	--	.48	--	--	--	--
0.49	--	--	--	--	--	--	--	--	--	--
--	.50	--	--	--	--	--	--	--	--	--
--	--	.32	--	.29	--	--	--	--	--	--
--	.32	--	--	--	--	--	--	--	--	--
--	--	.23	--	.19	--	--	--	--	--	--
--	--	--	--	--	--	--	--	--	--	--
--	.73	--	--	--	--	--	--	--	--	--
--	--	.78	--	.74	--	--	--	--	--	--
--	--	.50	--	.45	--	--	--	--	--	--
--	.61	--	--	--	--	--	--	--	--	--
--	--	.47	--	.44	--	--	--	--	--	--
--	.42	--	--	--	--	.37	--	--	--	--
--	.52	--	--	--	--	--	--	--	--	--
--	--	.38	--	.33	--	--	--	--	--	--
--	--	.57	--	--	0.44	.42	0.40	--	--	--
.77	--	--	0.58	--	--	.47	--	0.40	0.35	--
--	.53	--	--	--	--	.45	--	--	--	--
--	--	.56	--	.52	--	--	--	--	--	--
--	--	.65	--	.58	--	.51	--	--	--	--
--	--	.36	--	--	.27	.26	.24	--	--	--
.73	--	--	.65	--	--	.51	--	.36	.28	0.21
--	--	.92	--	.89	--	.82	--	--	--	--
1.00	--	--	1.00	--	--	.75	--	.63	.40	.33
--	--	.78	--	--	.70	.69	.68	--	--	--
1.00	--	--	1.00	--	--	1.00	--	1.00	.65	.54
--	--	.88	--	--	.84	.82	.81	--	--	--
.80	--	--	.64	--	--	.58	--	.46	.30	.22
--	--	.64	--	--	.56	.55	.53	--	--	--

Table 6.--*Water retention for mercury intrusion porosimetry method*

[Water retention, θ_v, in percent volumetric water content; matric potential, ψ_m, in bars. Tests done at U.S. Geological Survey petrophysics laboratory, in Golden, Colo.]

Sample 20AP		Sample 18AP	
θ_v	ψ_m	θ_v	ψ_m
0.2594	0.055	0.2747	0.088
.2589	.061	.2742	.711
.2578	.070	.2737	.984
.2574	.081	.2733	1.499
.2567	.103	.2723	2.399
.2559	.112	.2718	3.816
.2548	.129	.2705	4.770
.2536	.141	.2695	6.815
.2531	.152	.2685	8.177
.2523	.165	.2676	10.900
.2514	.179	.2636	15.330
.2487	.191	.2619	20.440
.2375	.301	.2551	24.530
.2255	.436	.2481	29.980
.2194	.572	.2191	37.480
.2149	.708	.1848	44.980
.2079	.981	.1686	49.060
.2039	1.253	.1577	51.790
.2003	1.499	.1500	54.520
.1983	1.772	.1436	57.240
.1956	2.181	.1424	61.330
.1907	2.590	.1385	63.380
.1886	3.135	.1324	68.150
.1866	3.680	.1257	74.960
.1837	4.634	.1235	81.770
.1822	5.452	.1192	87.230
.1795	6.815	.1183	95.400
.1733	14.310	.1087	102.200
.1716	17.720	.1067	109.000
.1702	20.440	.1050	115.800
.1678	27.260	.1017	122.700
.1643	40.890	.0999	129.500
.1604	51.790	.0982	136.300
.1481	59.970		
.1364	66.780		

Table 6.--*Water retention for mercury intrusion porosimetry method*--Continued

Sample 20AP	
θ_v	ψ_m
0.1318	72.230
.1254	79.050
.1193	87.230
.1156	92.680
.1114	102.200
.1090	109.000
.1066	115.800
.1043	124.000
.1026	129.500
.1012	136.300

Sample 8A		Sample 13A		Sample 19A	
θ_v	ψ_m	θ_v	ψ_m	θ_v	ψ_m
0.3306	0.057	0.3338	0.130	0.3265	0.053
.3300	.122	.3335	.302	.3256	.074
.3299	.174	.3318	.438	.3249	.089
.3296	.193	.3300	.574	.3245	.104
.3280	.329	.3281	.711	.3239	.115
.3252	.452	.3254	.847	.3231	.126
.3224	.574	.3243	.983	.3227	.142
.3204	.710	.3215	1.256	.3218	.152
.3147	.996	.3176	.567	.3209	.172
.3116	1.256	.3106	1.908	.3206	.182
.3088	1.499	.3057	2.290	.3168	.191
.3057	1.772	.2990	2.671	.3109	.301
.3031	2.072	.2962	2.889	.2950	.437
.3000	2.453	.2943	3.135	.2881	.573
.2972	2.862	.2900	3.544	.2836	.709
.2935	3.407	.2879	3.816	.2762	.845
.2905	3.952	.2842	4.361	.2694	1.363
.2865	4.770	.2820	4.770	.2628	1.935
.2836	5.452	.2798	5.179	.2592	2.453
.2798	6.406	.2771	5.806	.2561	3.135
.2777	6.951	.2732	6.815	.2517	4.116
.2749	8.177	.2711	7.251	.2491	4.770
.2713	9.540	.2673	8.859	.2467	5.452
.2681	10.900	.2620	11.580	.2436	6.815
.2630	13.630	.2593	13.630	.2383	10.900
.2586	16.350	.2526	17.040	.2362	13.630
.2546	19.080	.2479	19.080	.2334	17.720
.2493	23.170	.2422	21.810	.2314	21.810
.2442	27.260	.2350	24.530	.2292	27.260
.2369	32.710	.2286	27.260	.2267	32.710

Table 6.--*Water retention for mercury intrusion porosimetry method*--Continued

Sample 8A		Sample 13A		Sample 19A	
θ_v	ψ_m	θ_v	ψ_m	θ_v	ψ_m
0.2304	38.160	0.2181	30.670	0.2236	39.520
.2216	43.610	.2014	34.070	.2195	45.660
.2123	47.700	.1897	36.120	.2131	49.750
.2061	50.430	.1781	38.160	.2031	54.520
.1954	54.520	.1700	40.210	.1894	57.240
.1889	57.240	.1653	42.250	.1861	59.970
.1811	59.970	.1606	44.980	.1791	62.690
.1765	62.690	.1559	47.700	.1717	68.150
.1713	66.780	.1512	51.110	.1646	72.920
.1667	70.870	.1466	54.520	.1599	78.370
.1620	74.960	.1434	58.610	.1567	81.770
.1558	80.410	.1387	62.690	.1505	88.590
.1496	87.230	.1341	68.150	.1458	95.400
.1450	95.400	.1309	74.960	.1427	102.200
.1403	103.600	.1263	81.770	.1349	109.700
.1341	111.800	.1231	88.590	.1318	122.700
.1326	118.600	.1200	95.400	.1286	129.500
.1295	124.000	.1169	102.200	.1255	136.300
.1264	129.500	.1153	109.000		

Sample 14A		Sample 16A		Sample 11A	
θ_v	ψ_m	θ_v	ψ_m	θ_v	ψ_m
0.3476	0.046	0.3287	0.189	0.3259	0.057
.3459	.055	.3259	.302	.3253	.084
.3430	.070	.3230	.438	.3250	.121
.3402	.086	.3200	.574	.3246	.137
.3327	.103	.3172	.765	.3244	.154
.3284	.119	.3110	.982	.3241	.159
.3257	.125	.3077	1.132	.3238	.179
.3215	.138	.3044	1.255	.3235	.193
.3179	.152	.3004	1.417	.3222	.329
.3153	.164	.2951	1.635	.3211	.438
.3125	.178	.2931	1.772	.3190	.574
.3101	.191	.2910	1.908	.3158	.710
.2989	.299	.2887	2.058	.3133	.847
.2886	.435	.2852	2.208	.3106	1.011
.2817	.571	.2817	2.453	.3081	1.174
.2771	.707	.2779	2.617	.3043	1.363
.2674	.979	.2747	2.753	.3001	1.635
.2625	1.116	.2717	2.889	.2960	1.908
.2542	1.363	.2656	3.216	.2924	2.181
.2509	1.499	.2565	3.571	.2881	2.453

Table 6.--*Water retention for mercury intrusion porosimetry method*--Continued

Sample 14A		Sample 16A		Sample 11A	
θ_v	ψ_m	θ_v	ψ_m	θ_v	ψ_m
0.2477	1.635	0.2528	3.789	0.2858	2.726
.2409	1.908	.2482	4.143	.2817	3.135
.2339	2.181	.2467	4.416	.2778	3.544
.2295	2.453	.2407	4.770	.2732	4.089
.2239	2.726	.2333	5.343	.2694	4.634
.2187	3.135	.2303	5.724	.2666	5.179
.2150	3.407	.2244	6.188	.2619	6.133
.2107	3.816	.2184	6.706	.2589	6.815
.2069	4.089	.2110	7.373	.2511	9.540
.2035	4.498	.2035	8.177	.2438	12.270
.1991	5.179	.1902	9.540	.2383	14.990
.1948	5.997	.1693	11.580	.2330	18.400
.1905	6.815	.1619	13.630	.2270	21.810
.1818	7.496	.1530	17.040	.2195	26.580
.1790	10.220	.1455	20.440	.2099	31.350
.1732	12.270	.1336	24.530	.1965	36.800
.1689	14.310	.1172	28.620	.1826	40.890
.1660	16.350	.1038	34.070	.1725	42.930
.1602	20.440	.0934	39.520	.1658	44.980
.1530	25.900	.0845	45.660	.1579	47.700
.1415	32.710	.0770	51.790	.1516	50.430
.1271	37.480	.0726	57.240	.1453	53.150
.1127	40.890	.0666	65.420	.1422	55.880
.1040	43.610	.0636	72.230	.1375	58.610
.0982	46.340	.0607	79.050	.1328	61.330
.0910	50.430	.0562	88.590	.1281	65.420
.0867	54.520	.0547	95.400	.1233	69.510
.0824	58.610	.0532	102.200	.1202	73.600
.0795	64.060	.0502	109.000	.1155	79.050
.0752	70.870	.0487	115.800	.1108	84.500
.0708	79.050	.0487	122.700	.1076	90.630
.0680	87.230	.0473	129.500	.1029	98.130
.0651	95.400	.0458	136.300	.0982	107.700
				.0950	115.800
				.0919	122.700
				.0887	129.500
				.0872	136.300

STATISTICAL ANALYSES OF INTRINSIC PERMEABILITY DATA

For comparative analyses of permeability methods, it was indicated by using the Kolmogorov-Smirnoff test (Zar, 1984) that the intrinsic permeability data determined from the four methods were log-normally distributed. Correlations of the mean squared values and the variances squared gave coefficients of determination (r^2) >0.85. In addition, a fractile diagram of the data presented straight lines. Both of these analyses indicate log-normally distributed populations (Warrick and Nielsen, 1980). This distribution is skewed, as are the low-flow permeability data for all three methods. Determination of this distribution for these data indicates that the data are valid based on the idea that physical phenomena and parameters typically are characterized by distributions that are log normal. This is particularly true in geological settings and was shown to be true for permeability (Hammermeister, 1978). The geometric mean ($\bar{g}$):

$$[(X_1) \times (X_2) \times \ldots \times (X_n)]^{1/n}, \qquad (20)$$

weights the values so that one high value will not misrepresent the mean of the whole population.

In comparative analyses of subsamples involving very small sample sizes (n), arithmetic means ($\bar{x}$) are used for comparison along with standard deviations to illustrate the variation around the mean. In comparisons involving large sample sizes, the geometric mean ($\bar{g}$) and confidence intervals (standard deviations cannot be calculated for log-normally distributed populations) are used to compare permeability methods to more appropriately represent the populations. Because of uncertainties in the true distribution function for the data (for example, whether normal or log-normal), analyses based on the assumption of both normal and log-normal distributions are provided.

The difference between Calico Hills samples and the remaining samples is listed in table 3, which lists intrinsic permeability values for all samples. Calico Hills samples are designated as low flow. Also, using air permeability as an index, these samples exhibit a range of 0.01 (or 0.00) to 2.80 mD. This division is reasonable because the Calico Hills samples tend to have larger clay and zeolite contents and, therefore, probably have lower macroporosity. Also the clay and zeolites may interact with water and additionally contribute to the observed lower water flow rates. The only other sample indicating a lower flow rate is 10-A (0.09 mD), which has been classified as bedded-reworked tuff. Lithologic logs of the borehole from which the sample was taken describe this particular depth interval as argillic and zeolitic and include it as part of the Calico Hills to 1,835.7 feet. The remaining samples are considered to be high flow and exhibit a range of air permeability between 2.3 and 374.0 mD.

The permeability data listed in table 7 include means, standard deviations, and coefficient of variation (CV) of specific liquid permeability to water as a function of core-sample matrix description and provide a more detailed examination of the permeability data. Most noticeable is that the Calico Hills sample permeability values are, on the average, three orders of magnitude lower than all other sample permeability values.

When analyzed separately, the five different rock-unit types within the Calico Hills vary. This may indicate valid differences among rock-unit flows. Note also that vitric tuff samples exhibit the highest permeability values.

Table 7.--*Specific liquid permeability means, standard deviations, and coefficients of variation for core samples as a function of core matrix*

[n, number of samples used in analysis; CV, coefficient of variation; all analyses assume normally distributed populations]

Geologic unit	Core matrix description	n	Specific permeability to water (millidarcies)		
			Mean	Standard deviation	CV
Calico Hills	Vitric	2	0.291	0.290	0.997
	Devitrified, zeolitized	4	.030	.021	.690
	Zeolitized	8	.016	.007	.428
	Zeolitized, partially argillic	4	.006	.005	.428
	Bedded-reworked tuff	1	.010		
Base of Tiva Canyon Member	Vitric	2	50.01	49.99	1.00
	Vitric, partially argillic	1	145.90		
Yucca Mountain Member	Vitric	5	92.20	105.64	1.15
Pah Canyon Member	Vitric	4	17.59	19.35	1.10
Bedded-reworked tuff		5	5.89	7.09	1.20
Topopah Spring Member	Vitric	1	162.00		

The high-flow data in table 7 show much more variability as indicated by high coefficients of variation (CV), which is the standard deviation divided by the mean. Values of two samples from UE-25a #6 (see table 1), 4A and IV, although from samples in different formations, are much lower than the remaining sample values. In addition, there are three very low permeability values, two from UE-25 UZ #4: 4-4 from Pah Canyon Member and 4-7, bedded-reworked tuff from UE-25 UZ #5. No explanation for these low values can be offered at this time.

Statistical analyses of intrinsic permeability data are listed for four methods in table 8, including low- and high-flow samples, and under the assumption of both normally and log-normally distributed populations. The low-flow data are as expected, with the air permeability method measurements representing higher flow than the other three methods. The large variation in the high-flow data seems to complicate the arithmetic means, although the geometric means probably represent both the high- and low-flow data more accurately.

Table 8.--*Intrinsic permeability mean and standard deviation values*

[mD, millidarcies]

	Air permeability (mD)	Klinkenberg permeability (mD)	Nonpolar oil permeability (mD)	Specific permeability to water (mD)
		LOW FLOW		
Assumed normally distributed				
Mean ($\bar{x}$)	0.199	0.043	0.044	0.044
Standard deviation	.225	.056	.088	.124
Assumed log-normally distributed				
Mean ($\bar{g}$)	.129	.025	.007	.011
		HIGH FLOW		
Assumed normally distributed				
Mean ($\bar{x}$)	40.41	84.76	81.06	53.79
Standard deviation	111.78	105.55	105.76	76.99
Assumed log-normally distributed				
Mean ($\bar{g}$)	50.08	30.32	25.97	7.13

The Klinkenberg method for determining intrinsic permeability requires gas permeability measurements at each of several confining pressures. The change in permeability over the range of confining pressures used on 12 cores is listed in table 9. The values are related to core-matrix description. In the first six samples, there is a large percent change in permeability, 66 to 88 percent, over the range of confining pressures induced on those cores. The second six samples do not show large permeability changes. The integrity of the core matrix under pressure may be questioned when considering the large changes in sample permeability values. Zeolitized matrices occur in samples within the range of permeability changes whereas the three partially vitric cores all exhibited large changes in permeability with increased confining pressure. Differences in permeability values due to confining pressure may not pose a problem because this method accounts appropriately for in-situ overburden pressures.

Horizontal and vertical core intrinsic permeability values are listed in table 10. Means and standard deviations indicate little difference between data from vertical and horizontal core. The data also were regressed, and coefficients of determination (r^2) are listed. Correlations are fairly strong between the vertical and horizontal data for both the low- and high-flow samples.

Table 9.--*Reduction in Klinkenberg permeability values as a function of confining pressure for various rock matrix types*

Sample label	Depth (meters)	Confining pressure range (psi)	Percent change in permeability	Core matrix description
14A	1,880.3	300-900	88	Zeolitized
2P	1,398.2	300-900	82	Partially vitric
16A	1,932.5	300-400	80	Zeolitized
3P	1,516.3	300-900	70	Partially vitric
1P	1,329.0	300-900	67	Partially vitric
1A	1,785.6	50-200	66	Zeolitized, partially argillic
13A	1,792.3	50-200	29	Zeolitized
11A	1,700.0	300-900	22	Zeolitized, partially argillic
17A	2,076.0	300-750	19	Zeolitized
12A	1,756.9	300-900	17	Zeolitized
10A	1,801.5	300-900	9	Bedded, reworked
18A	2,168.6	300-750	7	Zeolitized

Table 10.--*Intrinsic permeability means and standard deviations, regression equations, coefficients of determination, and standard error of estimate for vertical permeability (y) for low- and high-flow core samples*

[Values represent all cores that had both vertical and horizontal measurements and include all determination methods; mD, millidarcies; n, number of samples; r^2, coefficient of determination; SEE, standard error of estimate for vertical permeability (y)]

		Vertical permeability (y) (mD)	Horizontal permeability (x) (mD)
Low flow	Mean	0.15	0.13
	Standard deviation	.26	.25
	n	19	8
High flow	Mean	40.96	42.78
	Standard deviation	61.88	74.30
	n	18	5

Regression equations		r^2	SEE
Low flow	y = 0.006 + 0.841 x	0.730	0.140
High flow	y = -3.161 + 1.122 x	0.873	28.230

Regressions established between the methods of intrinsic permeability determination for low- and high-flow samples are listed in table 11. Coefficient of determination (r^2) values express the proportion of the total variation in the values of the variable y that can be accounted for or explained by a linear relation with the random variable x. These values are very high for all regressions, which implies little need for expensive detailed measurements.

Table 11.--*Regressions of intrinsic permeability data for four methods of determination*

[Samples having data for all four methods were used, and all replicates were included. All values are in millidarcies]

Methods regressed (x versus y)	Regression equation	Coefficient of determination (r^2)	Standard error of estimate
Klinkenberg compared to air			
Low flow	y = -0.014 + 4.291 x	0.995	0.02
High flow	y = 17.247 + 0.861 x	.973	21.19
Klinkenberg compared to specific permeability to water			
Low flow	y = -0.074 + 2.489 x	.945	.05
High flow	y = -2.442 + 0.641 x	.999	3.24
Klinkenberg compared to nonpolar oil			
Low flow	y = -0.028 + 1.287 x	.983	.01
High flow	y = 1.291 + 0.909 x	.984	17.39
Specific permeability to water compared to air			
Low flow	y = 0.121 + 1.632 x	.944	.09
High flow	y = 20.938 + 1.335 x	.963	24.84
Specific permeability to water compared to nonpolar oil			
Low flow	y = 0.012 + 0.498 x	.967	.02
High flow	y = 4.609 + 1.421 x	.989	14.56

SUMMARY

The data obtained using four laboratory methods for the determination of permeability in rock cores showed considerable variability within the population. The variability probably was increased by the nature of sample selection. There was, however, a significant difference between sample values from the Calico Hills formation and all other rock units. On the average, Calico Hills intrinsic permeability values were smaller by three orders of magnitude.

The mean intrinsic permeability data for the four methods showed expected trends. Air permeability values were highest because they are not affected by fluid properties and interactions. Klinkenberg permeability values, which demonstrate ideal fluid permeability, were the next highest mean values. Nonpolar oil permeability values (which introduce the density and viscosity factors of fluids) and specific liquid permeability to water (which shows influences of formation water viscosity, density, and formation water-matrix interactions) were the lowest values.

There was virtually no difference between the means in intrinsic permeability values of horizontal and vertical cores. Regressions of horizontal compared to vertical core permeability values resulted in high coefficient of determination (r^2) values.

SELECTED REFERENCES

Amyx, J.W., Bass, D.M., Jr., and Whiting, R.L., 1960, Petroleum Reservoir Engineering: New York, McGraw-Hill Book Co., 609 p. (NNA.870831.0014)

American Society for Testing and Materials, 1985, Standard test method for determination of pore volume and pore volume distribution of soil and rock by mercury intrustion porosimetry, D4404-84: Annual Book of ASTM Standards, section 4, Construction, v. 4.08, Soil and rock: Building stones, p. 860-867. (NNA.900710.0185)

Blake, G.R., 1965, Bulk density, *in* Black, C.A., ed., Methods of soil analysis--Part 1, Physical and mineralogical methods, 1st ed.: Madison, Wisc., American Society of Agronomy, p. 383-390. (NNA.900208.0031)

Blake, G.R., and Hartge, K.H., 1986, Bulk density, *in* Klute, Arnold, ed., Methods of soil analysis--Part 1, Physical and mineralogical methods, 2d ed.: Madison, Wisc., American Society of Agronomy, p. 363-375. (NNA.900227.0043)

Brown, H.W., 1951, Capillary pressure investigations: American Institute of Mining and Metallurgical Engineers Transactions, v. 192, p. 67-74. (NNA.900710.0187)

Childs, E.C., 1940, The use of soil moisture characteristics in soil studies: Soil Science, v. 50, p. 239-252. (NNA.900710.0196)

Conca, J.L., and Lane, D.L., 1988, Determination of unsaturated transport parameters in whole rock and unconsolidated materials: Battelle, Pacific Northwest Laboratory, Chemical Systems Analysis Section, Richland, Wash., 6 p. (NNA.900710.0199)

Constantz, James and Herkelrath, W.N., 1984, A submersible pressure outflow cell for measurement of soil water retention and diffusivity from 5 to 95 °C: Soil Science Society America Journal, v. 48, no. 1, p. 7-10. (HQS.880517.2642)

Corey, A.T., 1986, Air permeability, *in* Klute, Arnold, ed., Methods of soil analysis--Part 1, Physical and mineralogical methods, 2d ed.: Madison, Wisc., American Society of Agronomy, p. 1121-1136. (NNA.900227.0043)

Hagoort, J., 1980, Oil recovery by gravity drainage: Society of Petroleum Engineers Journal, v. 20, no. 3, p. 139-150. (NNA.900710.0189)

Hammermeister, D.P., 1978, Water and anion movement in selected soils of western Oregon: Ph.D. thesis, Oregon State University, Corvallis, Oreg., 270 p. (NNA.900710.0190)

Hillel, Daniel, 1982, Fundamentals of Soil Physics: New York, Academic Press, Inc., 413 p. (HQS.880517.1776)

Hoffman, R.N., 1963, A technique for the determination of capillary pressure curves using a constantly accelerated centrifuge: Society of Petroleum Engineers Journal, v. 3, no. 3, p. 227-235. (NNA.900710.0191)
Klinkenberg, L.J., 1941, The permeability of porous media to liquids and gases, *in* Drilling and Production Practices: New York American Petroleum Institute, p. 200. (HQS.880517.1787)
Klute, Arnold, 1986, Water retention--laboratory methods, *in* Klute, Arnold, ed., Methods of soil analysis--Part 1, Physical and mineralogical methods, 2d ed.: Madison, Wisc., American Society of Agronomy, p. 635-662. (NNA.900227.0043)
Montazer, P., and Wilson, W.E., 1984, Conceptual hydrologic model of flow in the unsaturated zone, Yucca Mountain, Nevada: U.S. Geological Survey Water-Resources Investigations Report 84-4345, 55 p. (NNA.870519.0109)
Nimmo, J.R., Rubin, Jacob, and Hammermeister, D.P., 1987, Unsaturated flow in a centrifugal field--Measurement of hydraulic conductivity and testing of Darcy's law: Water Resources Research, v. 32, no. 1, p. 124-134. (NNA.870729.0073)
Owens, W.W., Parrish, D.R., and Lamoreaux, W.E., 1956, An evaluation of a gas drive method for determining relative permeability relationships: American Institute of Mining and Metallurgical Engineers Transactions, v. 207, p. 275-280. (HQS.880517.2815)
Purcell, W.R., 1949, Capillary pressures--Their measurement using mercury and the calculation of permeability therefrom: American Institute of Mining and Metallurgical Engineers Transactions, v. 186, p. 39-46. (NNA.890522.0236)
Richards, L.A., 1931, Capillary conduction of liquids in porous mediums: Physics, v. 1, p. 318-333. (NNA.890522.0282)
Scheidegger, A.E., 1957: The Physics of Flow through Porous Media: New York, Macmillan, 353 p. (NNA.900710.0192)
Scott, R.B., and Castellanos, Mayra, 1984, Stratigraphic and structural relations of volcanic rocks in drill holes USW GU-3 and USW G-3, Yucca Mountain, Nye County, Nevada: U.S. Geological Survey Open-File Report 84-0491, 127 p. (NNA.890804.0017)
Skuse, Brian, 1984, Capillary pressure measurements in reservoir rock cores using the centrifuge: Palo Alto, Calif., Applications Data, Beckman Institute, Inc., 4 p. (NNA.900710.0193)
Slobod, R.L., Chambers, Adele, and Prehn, W.L., Jr., 1951, Use of centrifuge for determining connate water, residual oil and capillary pressure curves of small core samples: American Institute of Mining and Metallurgical Engineers Transactions, v. 192, p. 127-134. (NNA.900710.0188)
Van Spronsen, Engel, 1982, Three-phase relative permeability measurements using the centrifuge method, *in* 3rd Joint SPE/DOE Symposium on Enhanced Oil Recovery: Tulsa, Society of Petroleum Engineers, p. 217-240. (HQS.880517.2894)
Warrick, A.W., and Nielsen, D.R., 1980, Spatial variability of soil physical properties in the field, *in* Hillel, Daniel, Applications of Soil Physics: New York, Academic Press, p. 319-344. (NNA.900710.0194)
Zar, J.H., 1984, Biostatistical Analysis, 2d ed.: New Jersey, Prentice-Hall, 718 p. (NNA.900710.0195)

NOTE: Parenthesized numbers following each cited reference are for U.S. Department of Energy OCRWM Records Management purposes only and should not be used when ordering the publication.

APPENDIX I

Graphs of Relative Permeability Determined Using Centrifuge and Gas-Drive Methods

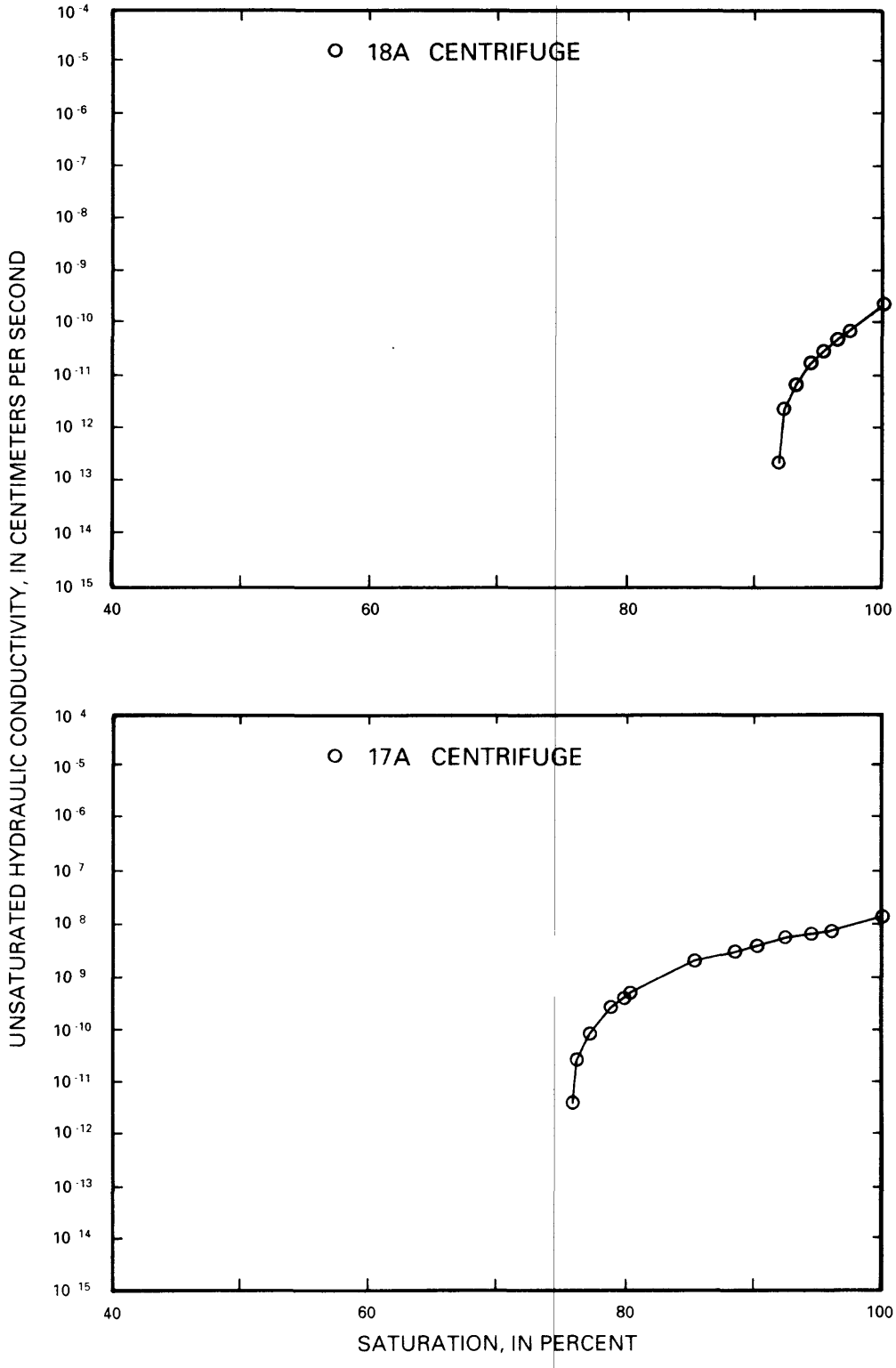

Figure I-1.--Relative permeability (unsaturated hydraulic conductivity) for samples 18A and 17A determined using centrifuge method.

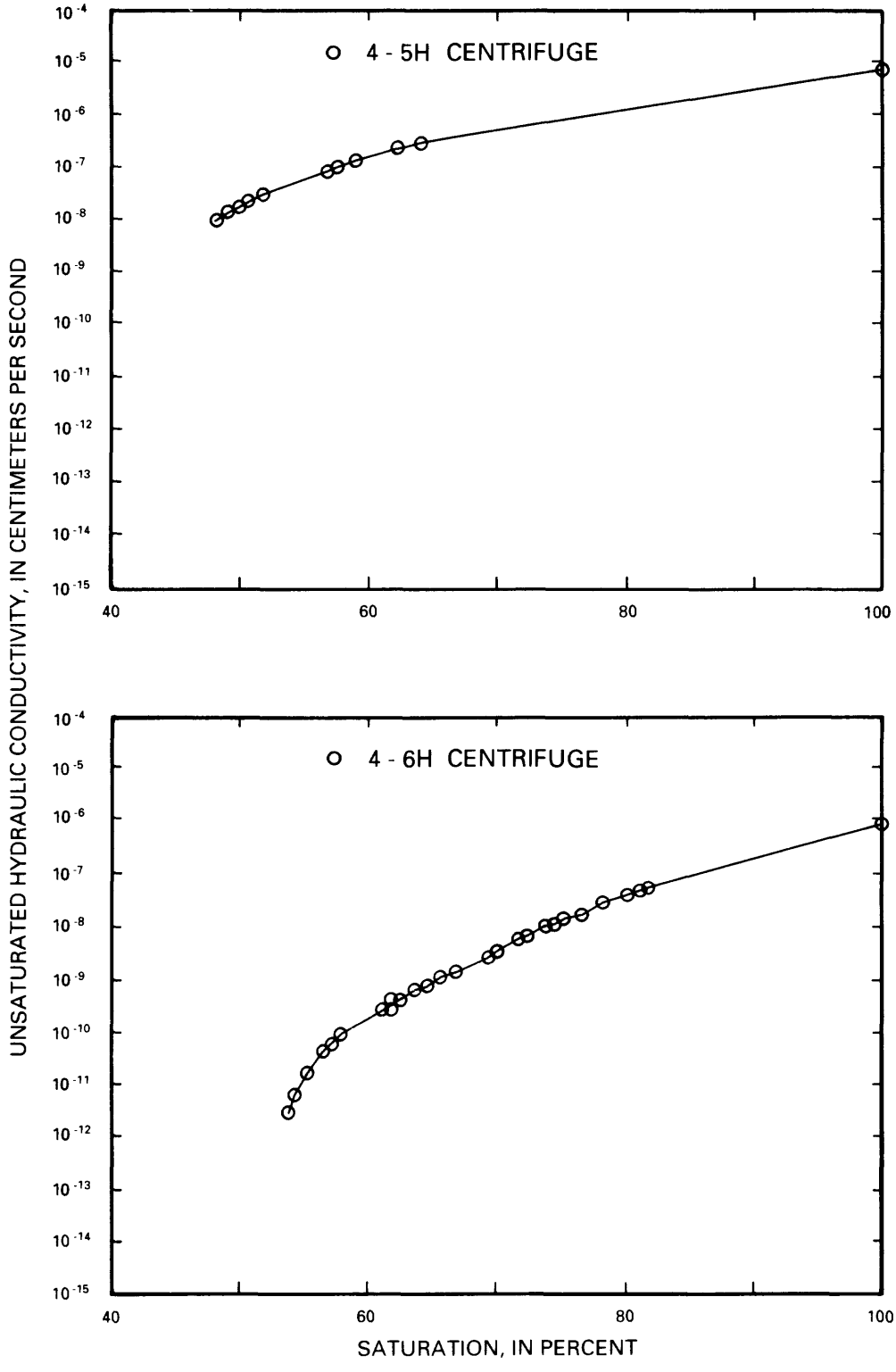

Figure I-2.--Relative permeability (unsaturated hydraulic conductivity) for samples 4-5H and 4-6H determined using centrifuge method.

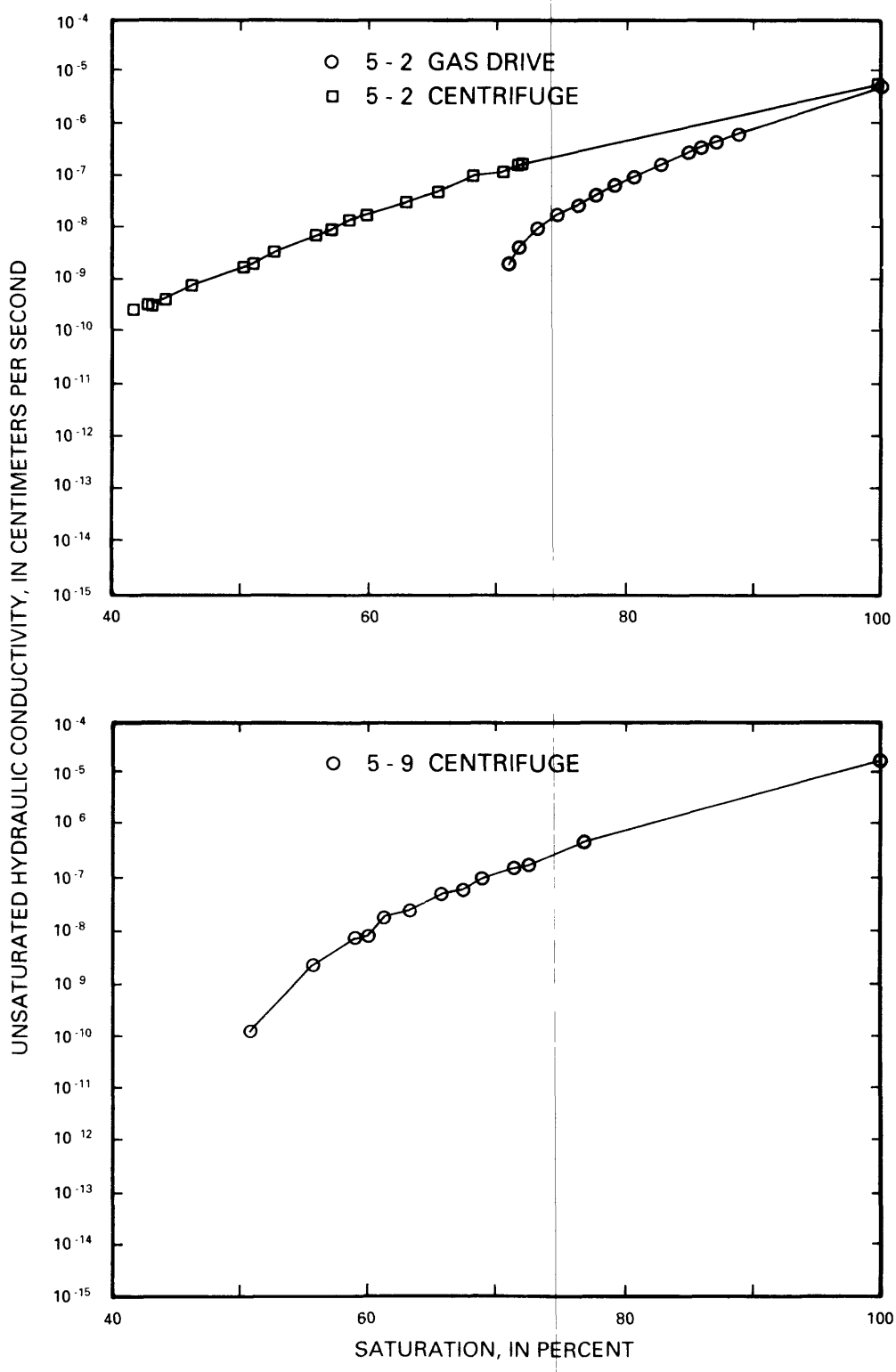

Figure I-3.--Relative permeability (unsaturated hydraulic conductivity) for sample 5-2 using centrifuge and gas-drive methods and for sample 5-9 determined using centrifuge method.

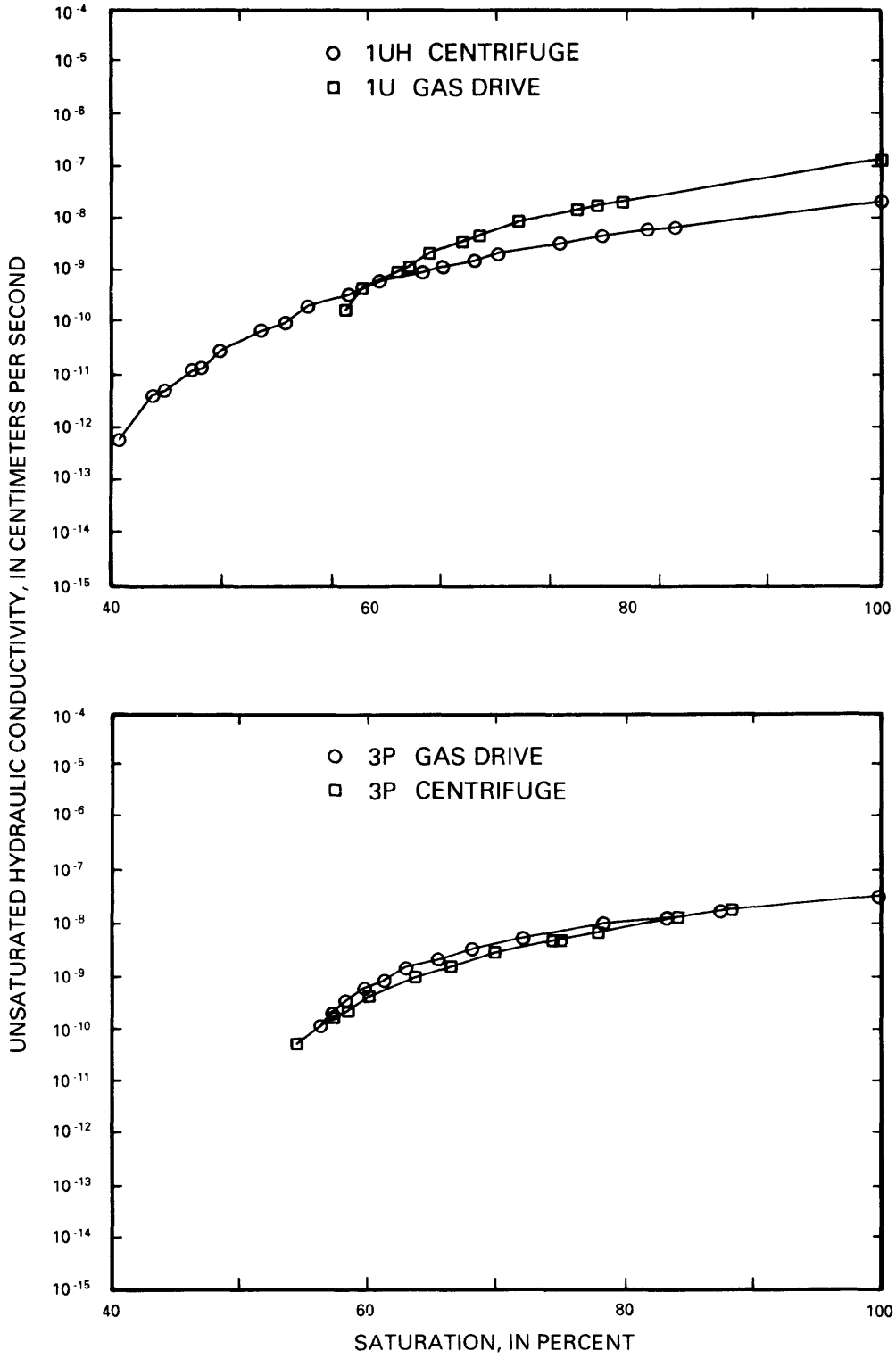

Figure I-4.--Relative permeability (unsaturated hydraulic conductivity) for samples 1UH and 3P determined using centrifuge method and for samples 1U and 3P using gas-drive method.

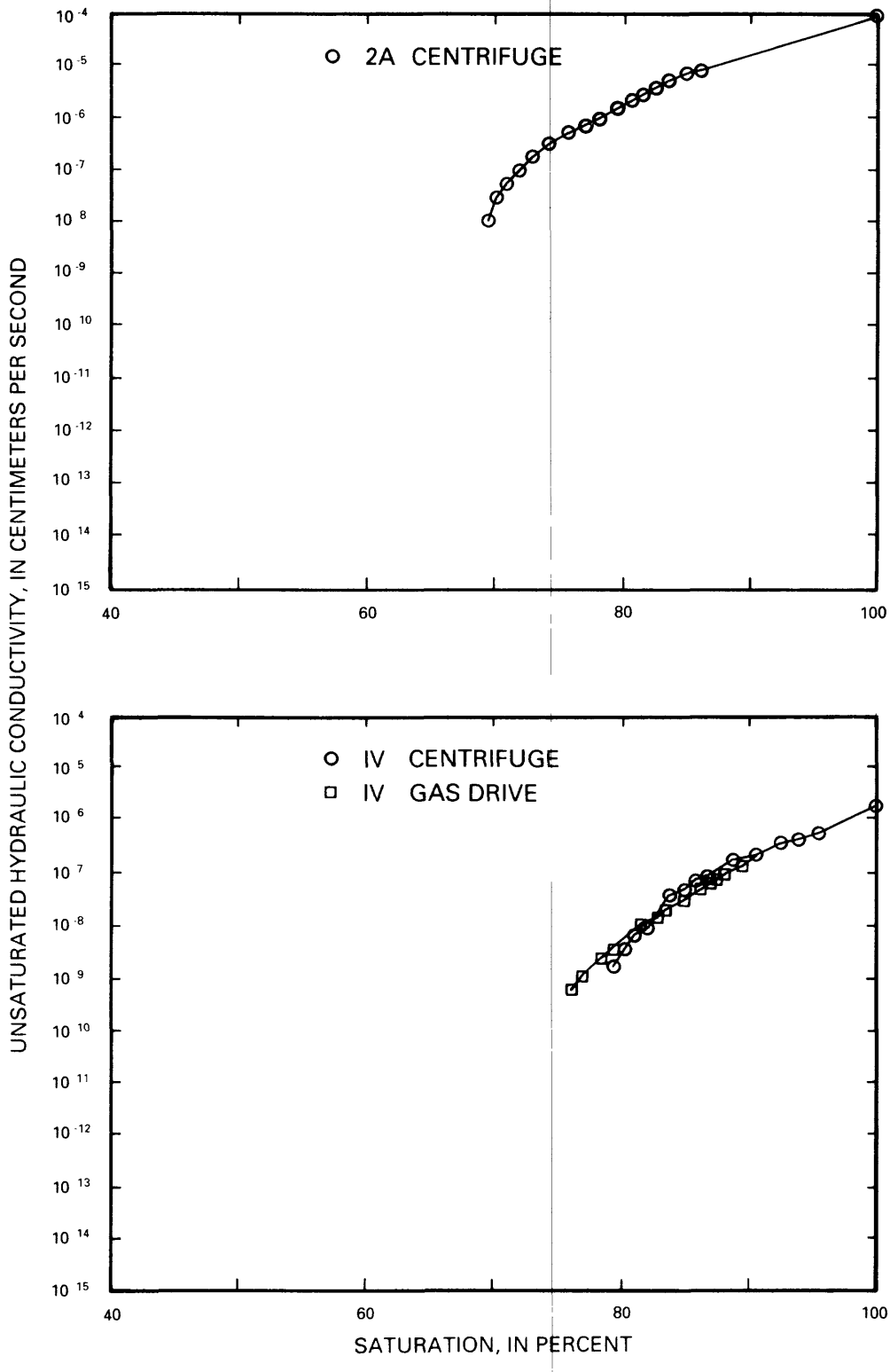

Figure I-5.--Relative permeability (unsaturated hydraulic conductivity) for sample 2A determined using centrifuge method and for sample IV using centrifuge and gas-drive methods.

APPENDIX II

Graphs of Water Retention:

II-1 through II-6. Centrifuge and Porous Plate Methods

II-7. Mercury Intrusion Porosimetry

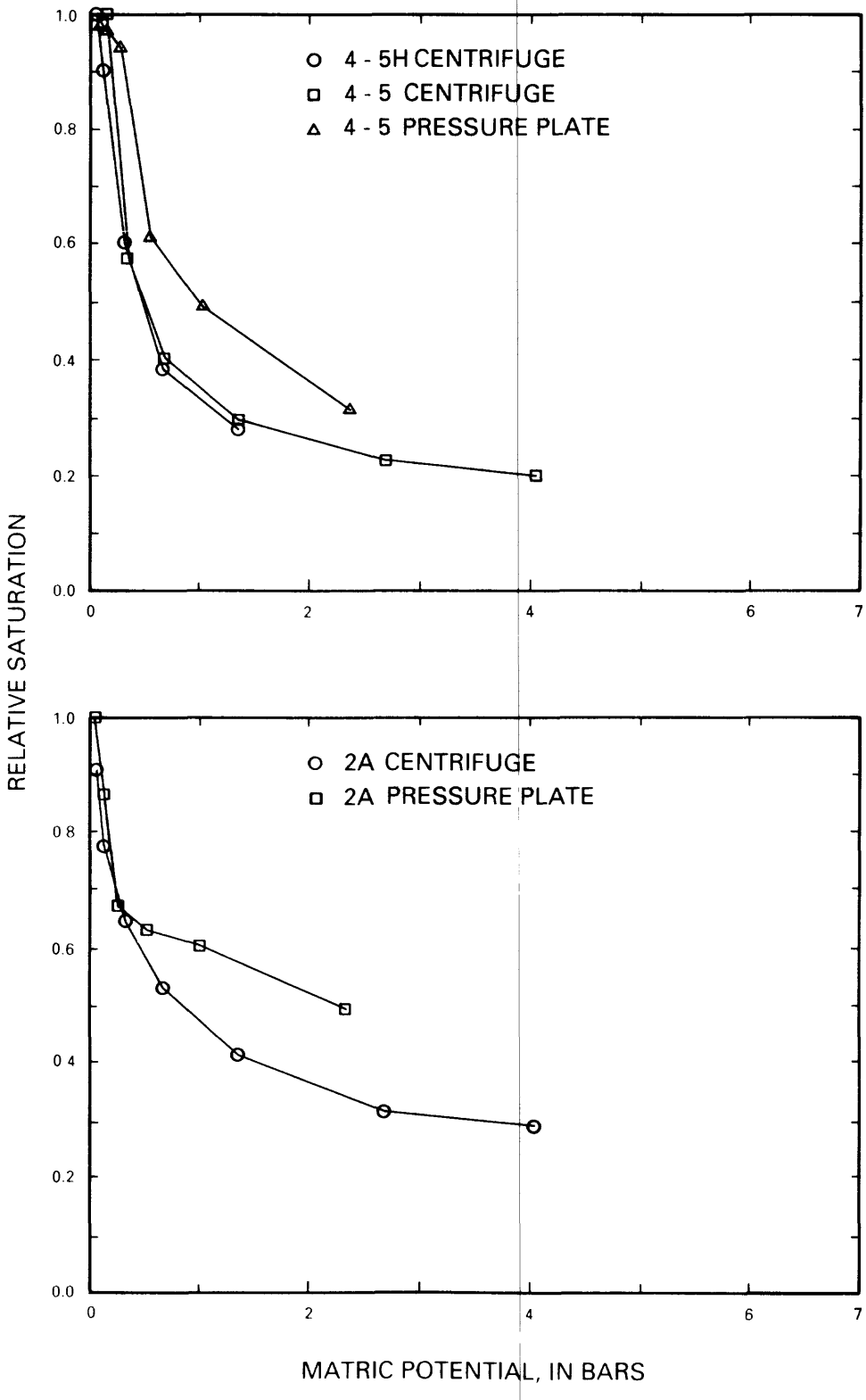

Figure II-1.--Water-retention curves for samples 4-5, 4-5H, and 2A determined using centrifuge and pressure plate methods.

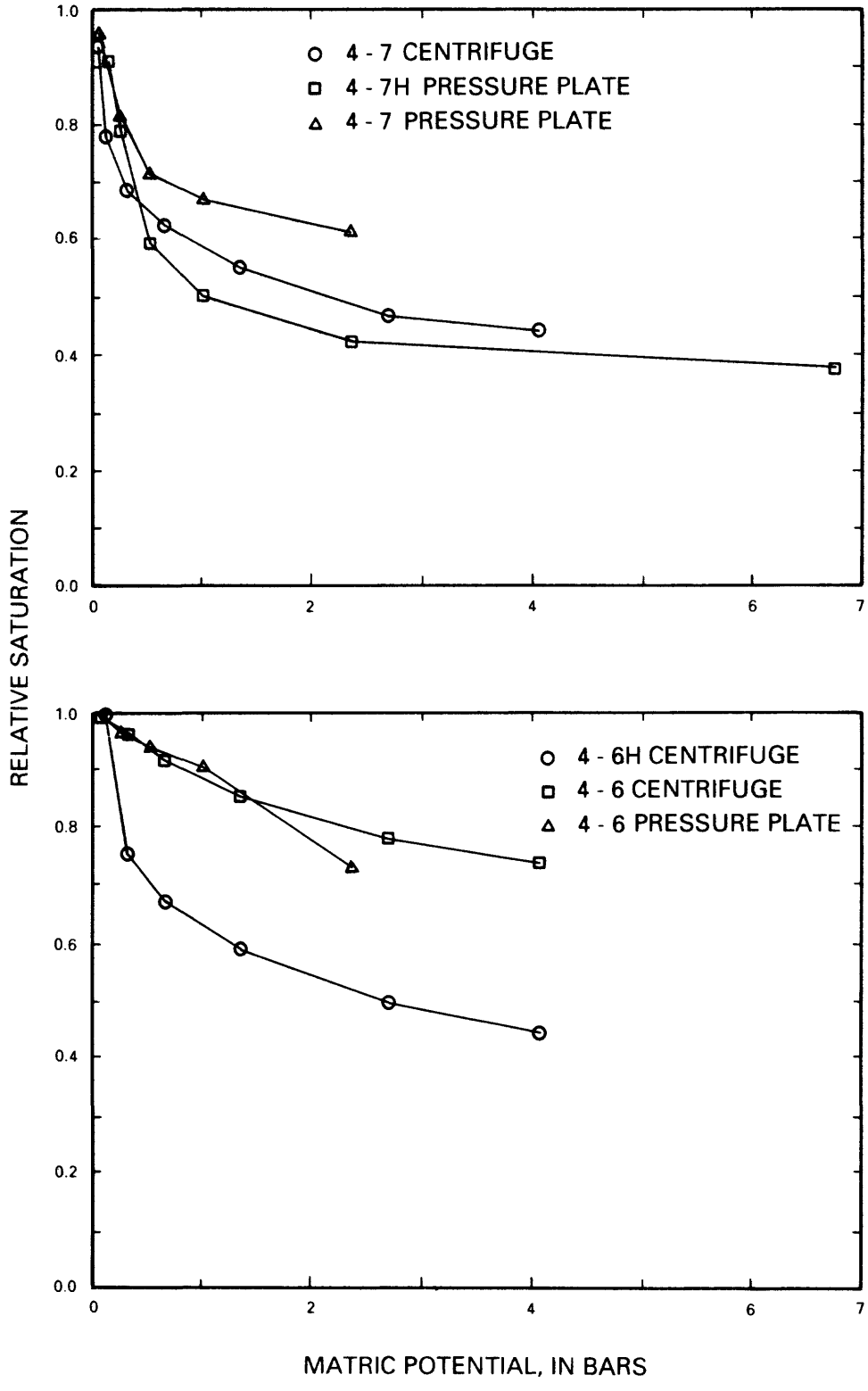

Figure II-2.--Water-retention curves for samples 4-7, 4-7H, 4-6, and 4-6H determined using centrifuge and pressure plate methods.

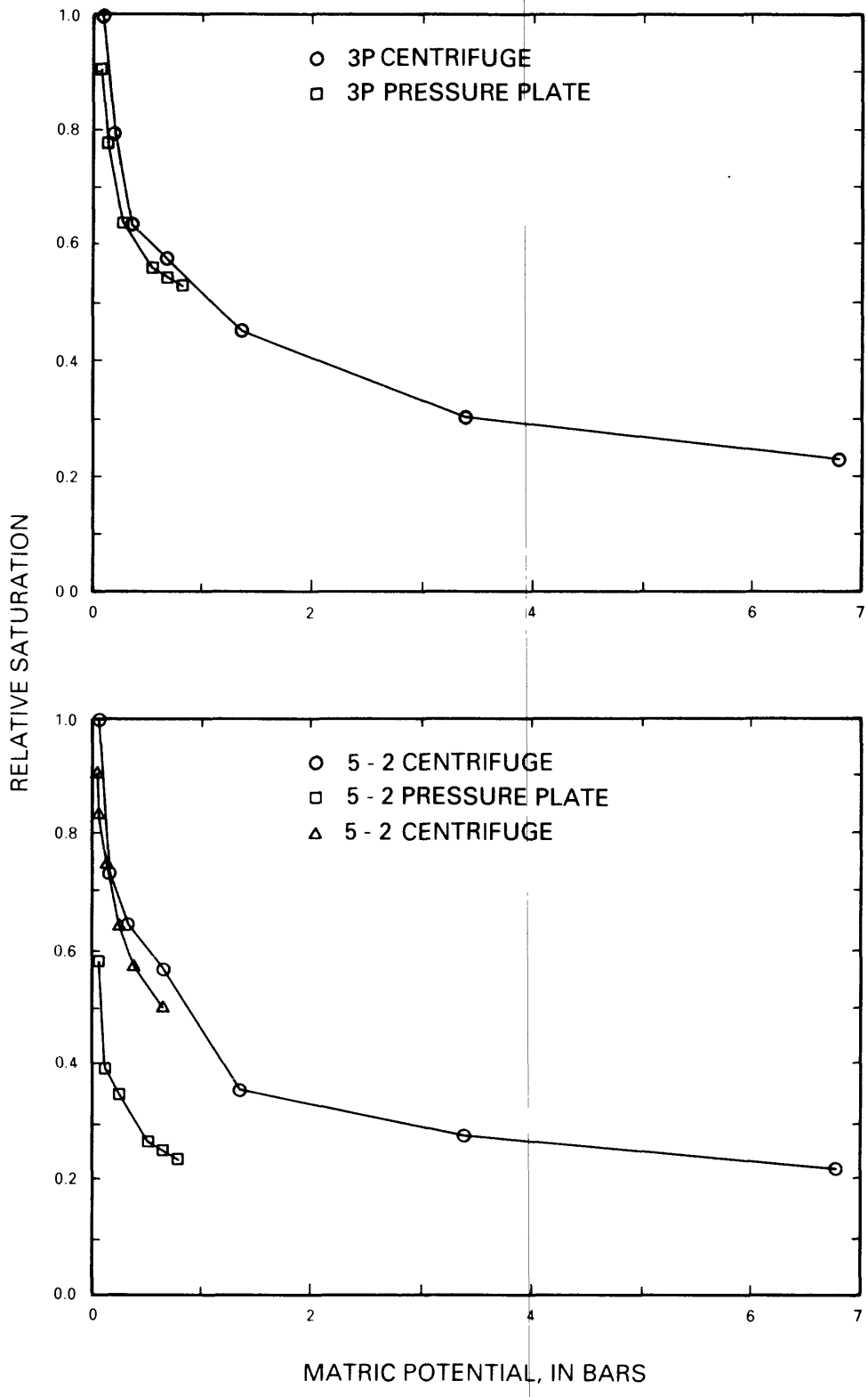

Figure II-3.--Water-retention curves for samples 3P and 5-2 determined using centrifuge and pressure plate methods.

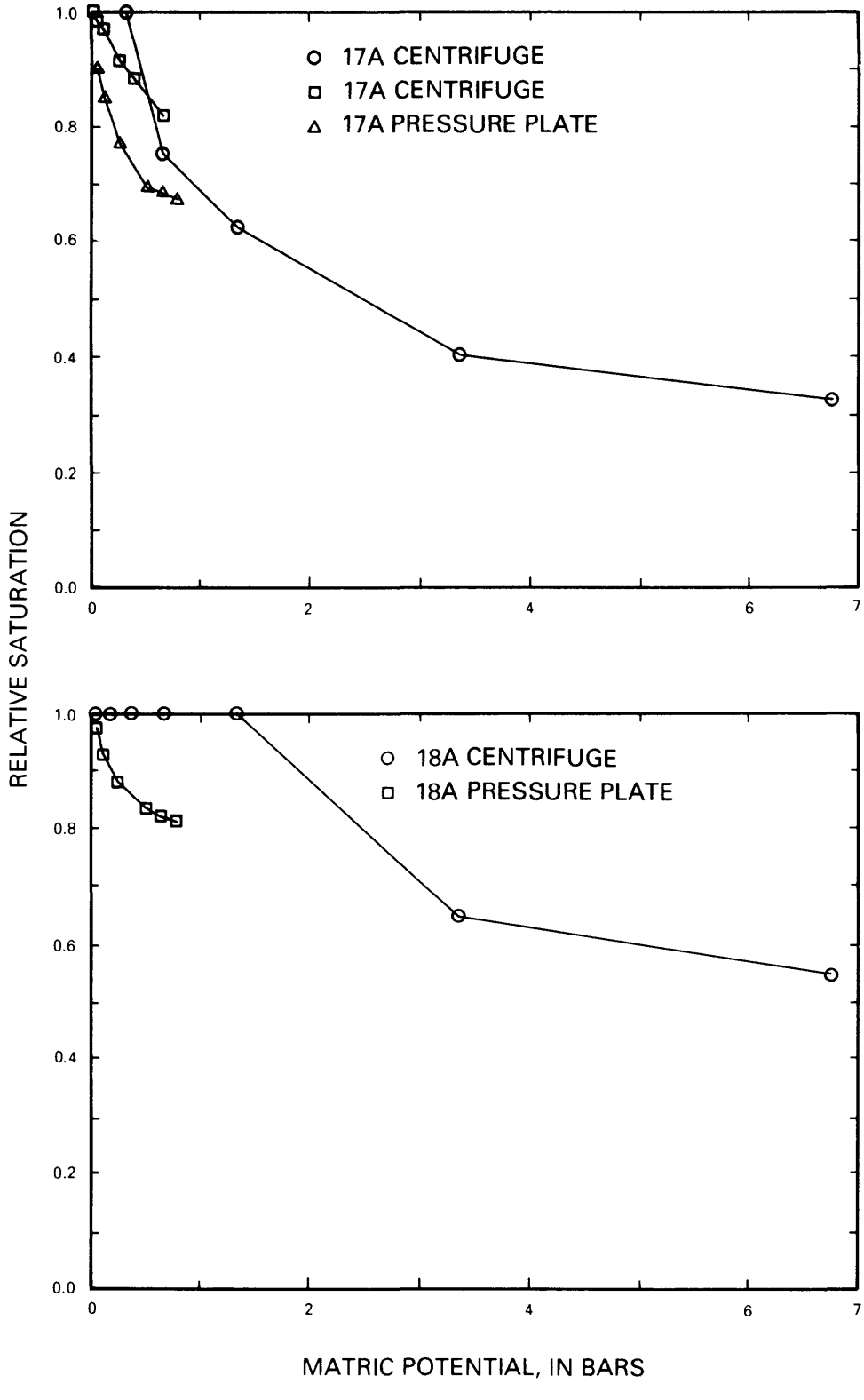

Figure II-4.--Water-retention curves for samples 17A and 18A determined using centrifuge and pressure plate methods.

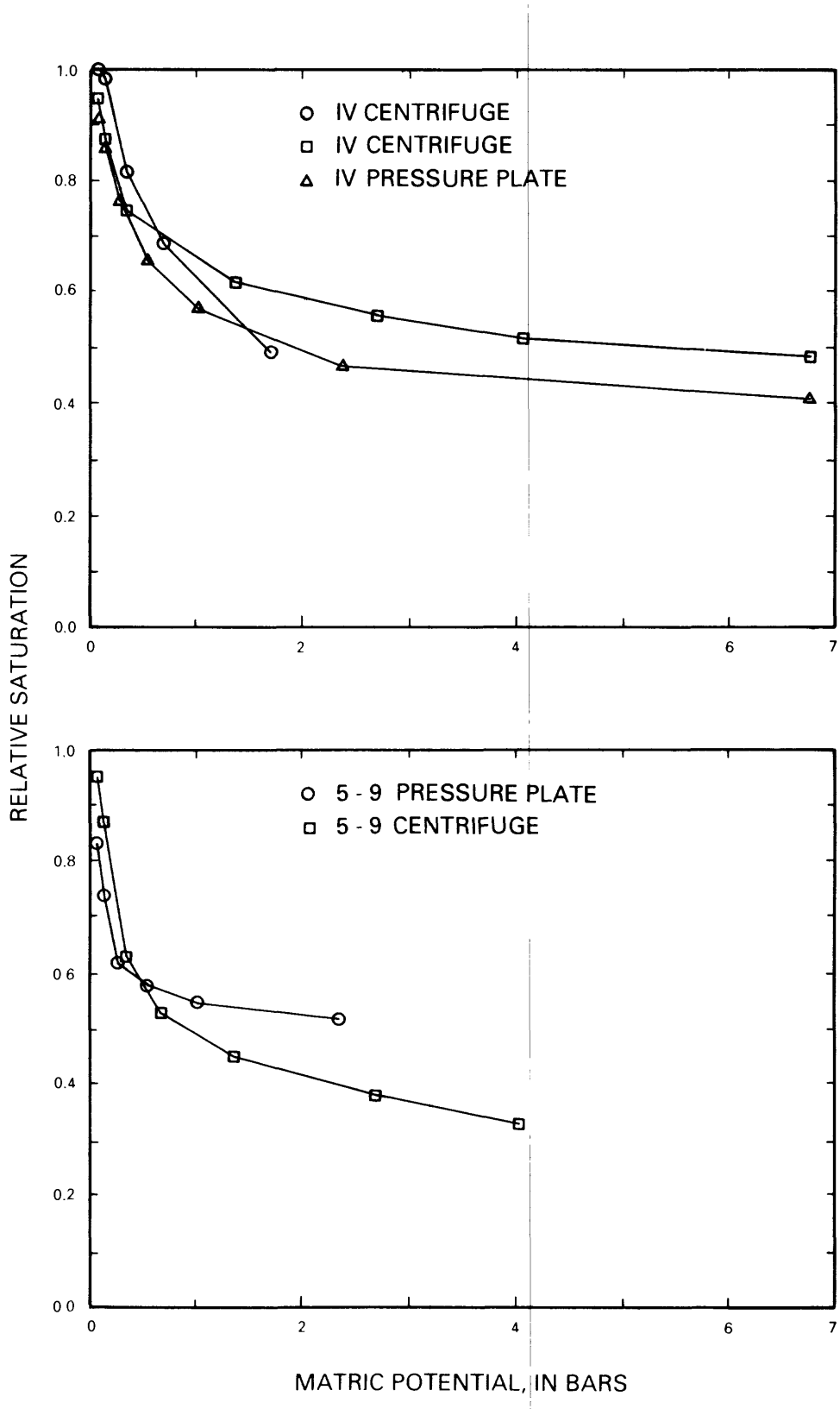

Figure II-5.--Water-retention curves for samples IV and 5-9 determined using centrifuge and pressure plate methods.

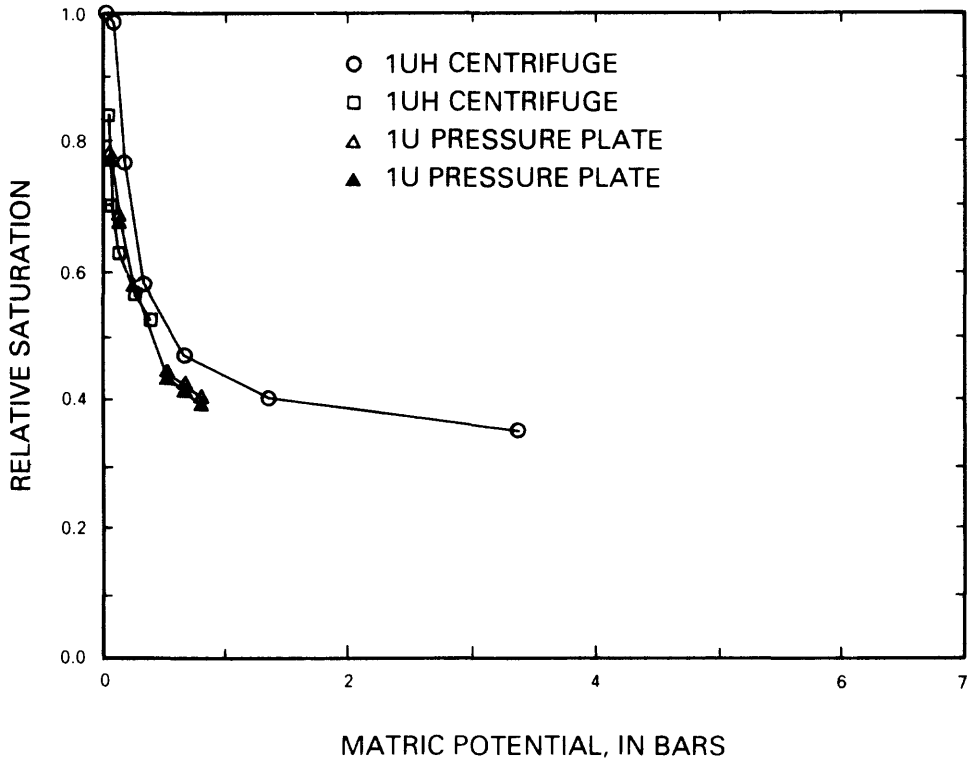

Figure II-6.--Water-retention curves for samples 1U and 1UH determined using centrifuge and pressure plate methods.

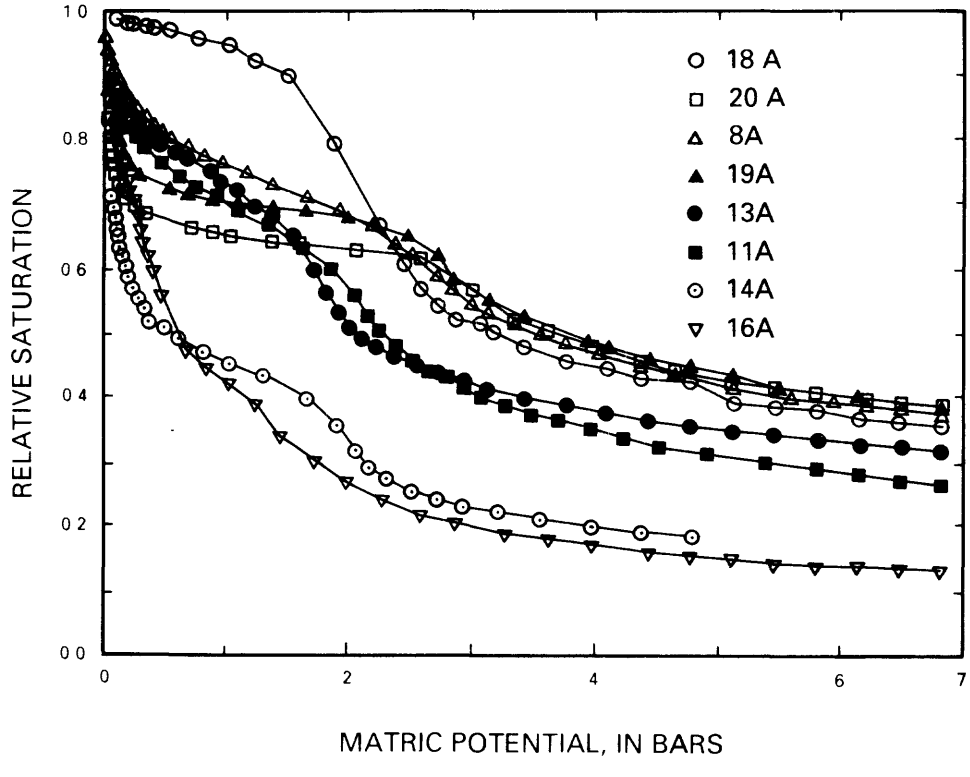

Figure II-7.--Water-retention curves calculated using mercury porosimetry for samples 18A, 20A, 8A, 19A, 13A, 11A, 14A, and 16A.

☆U.S. GOVERNMENT PRINTING OFFICE: 1991 - 576-003/45128